AD-A134 704

Applied Combustion Technology, Inc.

Expanded Ignition Effectiveness Tests of
Selected Igniter Materials with
Navy Propellants

Contract No. N00174-81-C-0453
Mod P00006

DISTRIBUTION STATEMENT A
Approved for public release;
Distribution Unlimited

Applied Combustion Technology, Inc.

ACT
APPLIED COMBUSTION
TECHNOLOGY, INC.
P.O. BOX [illegible]
ORLANDO, FLORIDA 32860
305-889-7537

FINAL REPORT

on

Expanded Ignition Effectiveness Tests of Selected Igniter Materials with Navy Propellants

Contract No. N00174-81-C-0453
Mod P00006

Performance Period

October 1982 - September 1983

Submitted to

Gun Systems Engineering
Naval Ordnance Station
Indian Head, MD 20640

Submitted by

A. Michael Varney and John Martino
Applied Combustion Technology, Inc.
P. O. Box 17885
Orlando, FL 32860

ACT-TR-8147

UNCLASSIFIED

SECURITY CLASSIFICATION OF THIS PAGE (When Data Entered)

REPORT DOCUMENTATION PAGE

READ INSTRUCTIONS BEFORE COMPLETING FORM

1. REPORT NUMBER: ACT-TR-8147	2. GOVT ACCESSION NO.: AD-A134 704
3. RECIPIENT'S CATALOG NUMBER	
4. TITLE (and Subtitle): Expanded Ignition Effectiveness Tests of Selected Igniter Materials with Navy Propellants	5. TYPE OF REPORT & PERIOD COVERED: Final Report Oct. 1982-Sept. 1983
	6. PERFORMING ORG. REPORT NUMBER: ACT-TR-8147
7. AUTHOR(s): Varney, A. Michael and Martino, John	8. CONTRACT OR GRANT NUMBER(s): N00174-81-C-0453 Mod P00006
9. PERFORMING ORGANIZATION NAME AND ADDRESS: Applied Combustion Technology, Inc. P. O. Box 17885 Orlando, FL 32860	10. PROGRAM ELEMENT, PROJECT, TASK AREA & WORK UNIT NUMBERS
11. CONTROLLING OFFICE NAME AND ADDRESS: Gun Systems Engineering Naval Ordnance Station Indian Head, MD 20640	12. REPORT DATE: September 1983
	13. NUMBER OF PAGES: 55
14. MONITORING AGENCY NAME & ADDRESS (if different from Controlling Office)	15. SECURITY CLASS. (of this report): Unclassified
	15a. DECLASSIFICATION/DOWNGRADING SCHEDULE

16. DISTRIBUTION STATEMENT (of this Report)

Distribution unlimited.

DISTRIBUTION STATEMENT A
Approved for public release
Distribution Unlimited

17. DISTRIBUTION STATEMENT (of the abstract entered in Block 20, if different from Report)

18. SUPPLEMENTARY NOTES

19. KEY WORDS (Continue on reverse side if necessary and identify by block number)

NACO Propellant	Black Powder	Ignition Effectiveness
NOSOL-318 Propellant	Boron Potassium Nitrate	Ammonium Perchlorate
NOSOL-363 Propellant	Magnesium-teflon-viton	
LOVA Propellant	Nitrocellulose	
Igniter Energy	Boron molybdenum trioxide	

20. ABSTRACT (Continue on reverse side if necessary and identify by block number)

Diagnostic ignition experiments have been conducted using a high-pressure flow through combustor to evaluate the ignition effectiveness of black powder, boron potassium nitrate, magnesium-teflon-viton, nitrocellulose, boron molybdenum trioxide and ammonium perchlorate with five propellants--NACO, NOSOL-318, NOSOL 363, LOVA, and PYRO. Twenty-one (21) series of experiments have been conducted to determine the

DD FORM 1473 1 JAN 73 EDITION OF 1 NOV 65 IS OBSOLETE

UNCLASSIFIED

SECURITY CLASSIFICATION OF THIS PAGE (When Data Entered)

20. ability of various igniter materials to ignite gun propellants beyond the immediate vicinity of the gun igniter--that is after filtering through and being cooled by an inert propellant simulant zone positioned between the igniter and the live propellant. The ignition effectiveness has been determined quantitatively by the amount of igniter thermal energy, based on its heat of explosion, required to ignite a propellant 50 percent of the time. Analyses and results are given which present the relative effectiveness of the igniter materials in terms of the different ignition stimuli (e.g., gases, liquids, and solids ratios).

PREFACE

This report summarizes project analyses and results for the experimental documentation of the ignition effectiveness of BP, $BKNO_3$, NC, MTV, $BMoO_3$, and AP igniter materials with NACO, NOSOL-318, NOSOL-363, LOVA, and PYRO propellants. The experimental program was conducted under Contract N00174-81-C-0453, Mod P00006 for the Naval Ordnance Station, Indian Head, Maryland from October 1982 to September 1983 by Applied Combustion Technology, Inc., Orlando, Florida. Mr. Charles Irish served as technical monitor for NOSIH and Dr. Michael Varney served as Principal Investigator for Applied Combustion Technology, Inc.

TABLE OF CONTENTS

LIST OF FIGURES

LIST OF TABLES

NOMENCLATURE

Symbol	Definition
A_e	Vent exit area
A_p	Propellant burning area
A_{sg}	Single grain surface area
A_{s1}	Total grain heat transfer area
A_{w1}	Bore wall area
AP	Ammonium perchlorate
B	Burning rate coefficient
$BKNO_3$	Boron potassium nitrate
$BMoO_3$	Boron molybdenum trioxide
BP	Black powder
cv	Control volume
C_{pcp}	Specific heat at constant pressure of condensed phase products
C_{pg}	Specific heat at constant pressure of igniter gases
C_{pub}	Specific heat at constant pressure of unburned material
C_s	Specific heat of solid
C_{vc}	Specific heat at constant volume
d_{p1}	Perforation diameter in region 1
D_e	Vent diameter
D_e^*	Compressible flow function defined in equation (2)
D_{g1}	Grain diameter in region 1
D_1	Wall bore diameter

Symbol	Definition
$\dot{E}_{cp}$	Condensed phase energy flux
E_e	Total exit energy
$\dot{E}_e$	Total energy flux
$\dot{E}_g$	Gas phase energy flux
E_{50}	Fifty percent firepoint energy
h_{cp}	Condensed phase enthalpy
h_{g1}	Heat transfer coefficient in region 1
h_{ub}	Enthalpy of unburned igniter material
h_{w1}	Heat transfer coefficient at bore surface
H_{cp}	Condensed phase enthalpy
H_g	Gas phase enthalpy
HOE	Heat of explosion
k_{g1}	Gas phase thermal conductivity
k_s	Thermal conductivity of solid
KE	Kinetic energy
L_{g1}	Grain length in region 1
m_{cp}	Mass of condensed phase products
$\dot{m}_{cp}$	Igniter mass flow rate: condensed phase
m_g	Mass of igniter gas
$\dot{m}_g$	Igniter mass flow rate: condensed phase
m_o	Igniter initial charge
m_r	Post-test mass residue
$\dot{m}_s$	Mass generation rate from solid
m_{ub}	Unburned igniter material vented with gas stream

Symbol	Definition
$\dot{m}_{ub}$	Igniter mass flow rate: unburned material
M_e	Exit Mach number
M_1	Mach number in region 1
MTV	Magnesium-teflon-viton
M_2	Region 2 Mach number
n	Burning rate index
n_{pl}	Number of perforations
n_v	Number of exit vents
n_1	Number of grains in zone 1
Nu_1	Nusselt number in region 1
NC	Nitrocellulose
P_c	Pressure in igniter cavity
Pr	Prandtl number
P_1	Pressure in region 1
Q_{wl}	Total heat transfer to wall in region 1
$\dot{Q}_{wl}$	Wall heat transfer rate in region 1
Q_1	Total heat transfer to grains
$\dot{Q}_1$	Heat transfer rate to grains
Re	Reynolds number
R_g	Gas constant
t	Time (independent variable)
T_c	Chamber temperature
T_e	Gas phase vent exit temperature
T_o	Initial temperature

Symbol	Definition
T_p	Adiabatic flame temperature of igniter material at constant pressure
T_s	Grain surface temperature
T_{so}	Initial soak temperature
T_w	Wall temperature
T_1	Temperature in region 1
V_e	Igniter vent exit velocity
$\bar{V}_{g1}$	Individual grain volume
V_1	Velocity in region 1
$\bar{V}_1$	Bore volume in region 1
α_s	Thermal diffusivity of grain
β	Ratio of condensed phase products to gas phase products
γ	Ratio of specific heats
ε_1	Inert bed void fraction, Zone 1
ρ_p	Propellant density
ρ_s	Density of solid
ρ_1	Gas phase density in region 1
τ_{final}	Igniter action time
μ	Gas viscosity

Sub-scripts	
c	Igniter cavity
cp	Condensed phase
g	Gas phase
s	Solid

Symbol	Definition
w	Wall
1	Inert simulant region
2	Live propellant region
3	Exit region

1.0 INTRODUCTION

1.1 Background

Diagnostic experiments have been conducted to characterize the ignition effectiveness of selected igniter materials with Navy propellants under simulated gun firing conditions. Experimental firings have been conducted with a high pressure, flow through combustor to determine the ability of various igniter materials to ignite gun propellants beyond the immediate vicinity of the gun igniter--that is after filtering through and being cooled by an inert propellant simulant zone positioned between the igniter vents and the live propellant. Ignition effectiveness is determined quantitatively by the amount of igniter thermal energy, based on its heat of explosion, required to ignite a propellant 50 percent of the time. With the determination of the ignition effectiveness of a variety of ignition materials which have a wide range in their distribution of physical states, one can in principle determine the more effective combinations of physical states (hot gases, vapors, liquids, and solids), heat of explosion, flame temperature, and oxidizer content leading to effective igniter characterization. Successful implementation of this approach would then provide a basis for searching for better igniter materials for existing primers, or for new igniter designs for new guns, or for existing guns with difficult ignition conditions.

1.2 Summary

In previously completed efforts (Ref. 1), Applied Combustion Technology, Inc. conducted seventeen (17) series of ignition effectiveness tests with NACO, NOSOL-318, and NOSOL-363 propellants using BP, $BKNO_3$, MTV, and $BMoO_3$ igniter materials. The previous results, presented in References 1 and 2, are complemented by twenty-one (21) additional experimental series in the current project, bringing the total data base to 37 Bruceton-style ignition effectiveness test series (one series for $BMoO_3$ was inconclusive and is not included in the data reduction).

During the current project, Applied Combustion Technology, Inc. has achieved the following goals:

1. Conducted twenty-one (21) series of ignition effectiveness tests with NACO, LOVA, NOSOL-318 and PYRO propellants using BP, $BKNO_3$, NC, MTV, $BMoO_3$, and AP igniter materials.
2. Conducted Bruceton sensitivity analyses to determine 50 percent firepoint ignition energy levels for all 37 series of ignition effectiveness test data using new, experimentally determined NOSIH heat of explosion data.
3. Developed an analytical data reduction model to correct igniter charge energy levels for convective losses to an inert simulant packed bed.

Comparisons between experimentally determined data and theoretical calculations are presented herein with test data, analyses, and conclusions. Of the data acquired, the firing results of NACO and LOVA propellants are the most complete. A review of the composite firing data suggests that igniter product gas phase mass fractions on the order of 30-50 percent are essential for propellant ignition at minimum input pressure levels. Further, the results obtained suggest the importance of igniter product liquid phase mass fractions for achieving an in-depth propellant ignition boundary. LOVA 50 percent ignition energy levels were observed to be 2-3 times greater than observed for NACO propellant. LOVA ignition energy requirements were found to be significantly reduced by the presence of oxidizer species in the igniter (AP); LOVA ignition sensitivity with AP was equivalent to the energy requirements for the easy-to-ignite NACO propellant with conventional materials.

2.0 EXPERIMENTAL

2.1 Hardware Description

Ignition effectiveness experiments have been conducted using a high pressure, flow through combustor, Figure 2.1. The igniter assembly is designed to accommodate a 20 mm electric primer which is used to initiate up to one cubic inch (16 cm^3) of pyrotechnic material; igniter discharge into the combustion chamber bore is via five axial vents arranged symmetrically about a centerline vent. The internal volume of the combustion chamber is 620 cm^3, minus the volume of the igniter vent assembly, and is equipped with six access ports to monitor pressure response and/or light generation during propellant ignition and flame spreading. Aft end closure of the combustion chamber is achieved by an axially ported insert which is sized to permit pressure buildup during propellant ignition and adequate venting during combustion. A complete hardware description is provided in Reference 3.

2.2 Experimental Procedures

2.2.1 Igniter Calibration Tests

Each of the igniter materials utilized in the ignition effectiveness tests was evaluated for output performance (bed input) by installing a pressure transducer into the centerline axial vent and firing into the IECD bore, which had been filled with inert simulant to provide propellant back pressure effects on the igniter outflow. A three point curve was generated for each igniter material as a function of igniter charge loading for the igniter masses shown in Table 2.1.

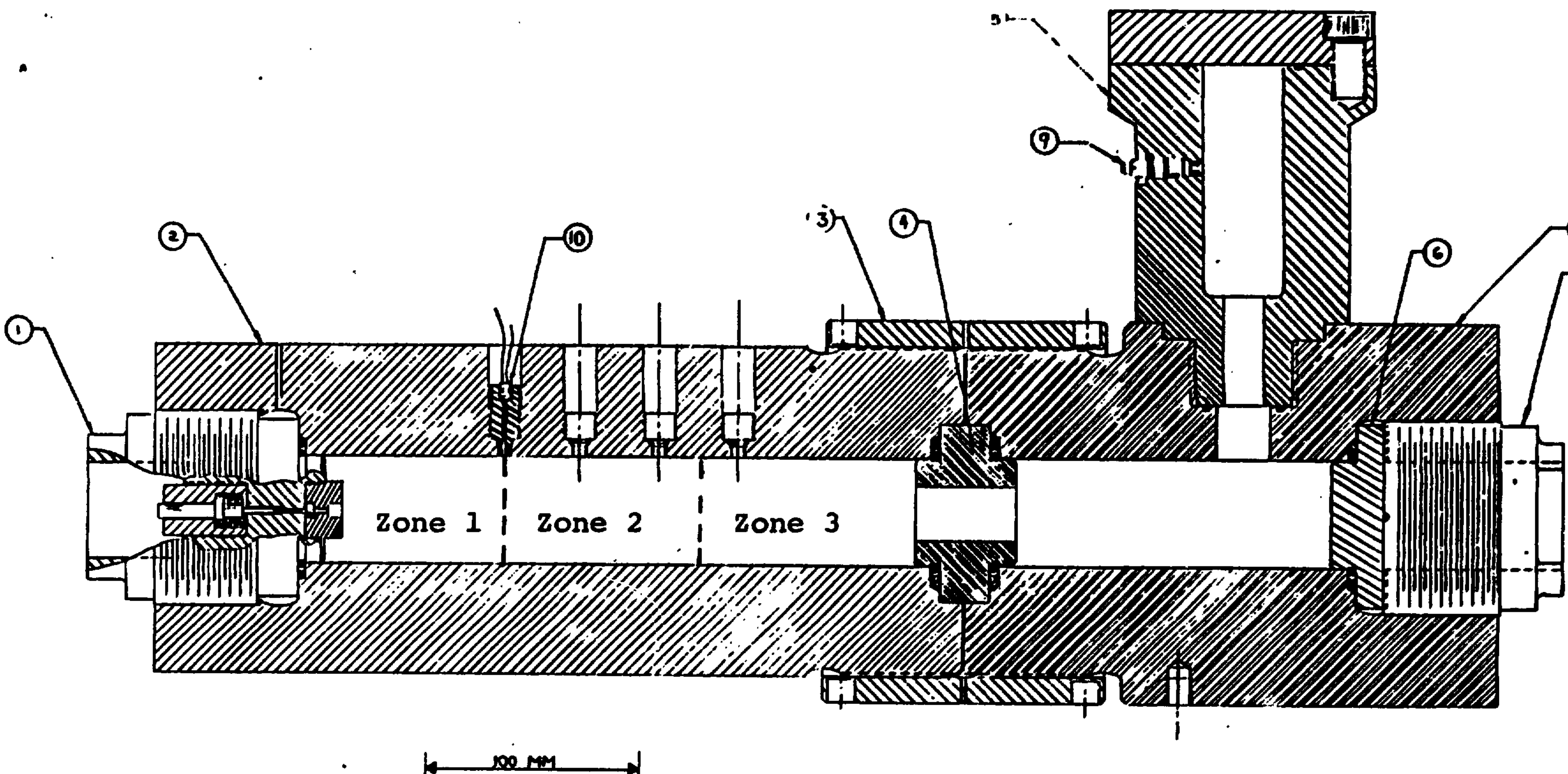

NOTE: Zone 1 ~ Inert Simulant Bed Length (L_1)
Zone 2 ~ Live Propellant Bed Length (L_2)
Zone 3 ~ Inert Simulant Bed Length (L_3)

Fig. 2.1 Applied Combustion Technology, Inc. ASSEMBLY IECD

Table 2.1 Igniter Calibration Test Series

Igniter Charge Mass (g)

BP	$BKNO_3$	NC	MTV	AP
1.27	0.90	1.10	1.10	1.24
2.78	1.80	2.80	1.94	2.59
5.75	2.85	4.30	2.95	4.0

Each igniter calibration record was utilized for analytical treatment of the ignition effectiveness data and is presented in Section 3.0, Data Analysis.

2.2.2 Ignition Effectiveness Tests

Ignition effectiveness tests were conducted using the IECD with fixed zone lengths of inert simulant separating the igniter vent exit plane and the live propellant zone, as shown in Figure 2.2. Diagnostic firings were conducted for selected combinations of six igniter materials, five propellants, and four inert simulant zone lengths, as shown in Table 2.2. Seventeen (17) series of tests were previously conducted (Ref. 1) and twenty-one (21) new series of test data have been generated in the current project; data and data analyses for 37 series of tests is presented herein. Igniter material characterization and propellant characterization are presented in Tables 2.3 and 2.4, respectively. Heat of explosion values were experimentally determined by NOSIH using a Parr bomb pressurized with nitrogen to 25 atmospheres. Other values shown in Table 2.3 were calculated using NASA-Lewis chemical equilibrium calculations for a chamber pressure of 500 psia expanding to 14.7 psi. Ignition effectiveness was determined quantitatively by the amount of thermal energy, based on its heat of explosion, required

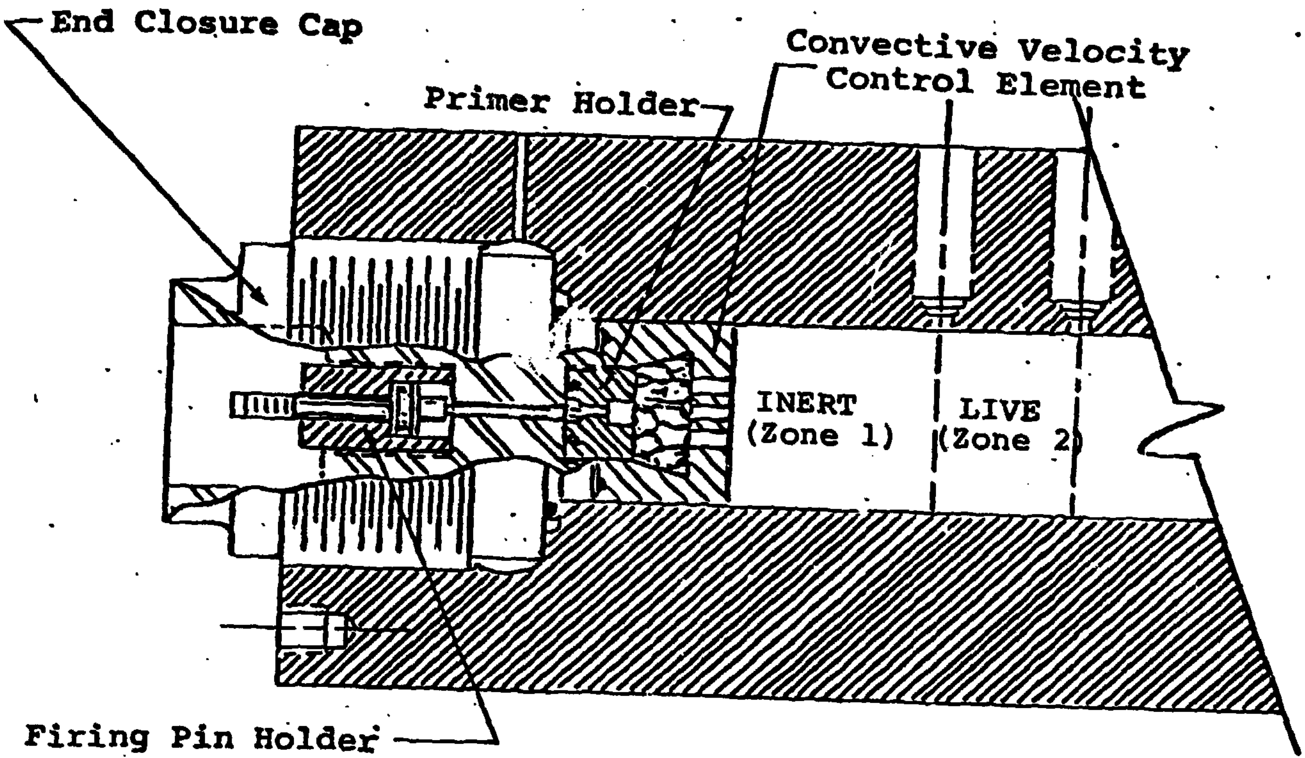

Figure 2.2 Igniter Assembly and Typical Test Configuration

Table 2.2
IECD BRUCETON TEST MATRIX

Bed Length 0.0"	Igniter Material					
Propellant	BP	BKN	NC	MTV	$BMoO_3$	AP
NACO						
N318						
LOVA	X	X	X	X	X	X
N363						
PYRO						

Bed Length 1.0"	Igniter Material					
Propellant	BP	BKN	NC	MTV	$BMoO_3$	AP
NACO	X	X	X		X	
N318		X	X			
LOVA	X	X		X		
N363						
PYRO						

Bed Length 1.5"	Igniter Material					
Propellant	BP	BKN	NC	MTV	$BMoO_3$	AP
NACO	X	X	X	X	X	
N318	X	X	X	X		
LOVA	X	X	X	X		X
N363	X	X	X	X		
PYRO			X			

Bed Length 2.0"	Igniter Material					
Propellant	BP	BKN	NC	MTV	$BMoO_3$	AP
NACO	X	X	X	X		
N318						
LOVA						
N363						
PYRO						

Table 2.3 Igniter Material Characterization (NASA-Lewis)

Item	Igniter Material[1] BP	BKNO$_3$	NC	MTV	AP
Density (g/cm^3)	1.6	1.4	1.2	1.5	1.9
HOE (Cal/g)	709	1495	920	1540	826
Flame Temperature, T_p (°K)	1930	2890	2350	2650	1400
Gas Constant ($ft\text{-}lb_f/lb_m\text{-}^\circ R$)	28	25	62	26	55
Specific Heat (C_p, $Btu/lb_m\text{-}^\circ R$)	.62	1.61	.46	1.01	.36
Molecular Weight (Products)	56	63	25	60	28
Ratio of Sp Heats (γ)	1.11	1.08	1.22	1.09	1.26
Products Mass Fraction (%)					
Vapor-Solid	1.0	54.9	0	39.6	0
Liquid-Solid	40.9	3.5	0.6	47.7	0
Solid	0	16.9	0	12.4	0
Total Solid at 14.7 psi	41.9	75.3	0.6	99.7	0
Gas	54.8	24.7	90.2	0.3	75.6
Total	96.7*	100.0	90.8*	100.0	75.6*

*Balance Water Vapor

[1]Material	Composition
1-BP	Black powder (ffg)
2-BKNO$_3$	23.7% B, 70.7% KNO$_3$, 5.6% Laminac
3-NC	IMR 4895
4-MTV	Magnesium-Teflon-Viton (54%/30%/16%)
5-AP	Ammonium perchlorate

Table 2.4 Propellant Geometrical Characterization

Propellant[1]	Grain Dimensions Dia (in)	Grain Dimensions Length (in)	Charge (g)	Number of Grains	Bed Length (in)	Bed Porosity (d'less)
LOVA[2]	.20	.28	40	187	0.9	.41
NACO	.24	.42	40	97	1.0	.41
NOSOL-318	.32	.68	40	33	1.1	.48
NOSOL-363	.44	.96	40	12	1.0	.45
PYRO	.32	.75	40	28	1.0	.46
M26	.53	1.25	40	6	0.9	.40
Inert Simulant	.30	.62	0	0	0	-
			33	33	1.0	.50
			52	52	1.5	.50
			74	74	2.0	.50

[1] Seven (7) perf grains

[2] CAB/ATEC

to ignite the propellant 50 percent of the time as determined by an up-and-down (Bruceton) test technique (Reference 4). Each test grouping included a series of pre-Bruceton shots to determine the approximate 50 percent firepoint as the starting energy level for a limited Bruceton series consisting of ten (10) shots each. Test data for each event included a Yes/No fire observation and an in-bore oscilloscope record of the pressure-time profile resulting from the igniter input and subsequent propellant combustion. A complete run log of the IECD ignition diagnostic tests is included as Appendix A, where firing data have been arranged in order to ascending inert simulant bed length from 0.0 inches to 2.0 inches.

2.3 Fifty Percent Firepoint Results

2.3.1 Fifty Percent Firepoint Data

Twenty-one (21) series of Bruceton tests were conducted in the current project to evaluate the ignition effectiveness of BP, $BKNO_3$, NC, MTV, $BMoO_3$, and AP igniter materials with NACO, LOVA, NOSOL-318, and PYRO propellants for selected zone one inert bed thicknesses ranging from 0.0 inches to 2.0 inches. Initial data reduction consisted of reading the in-bore oscilloscope records of each shot to record pertinent pressure-time data, as indicated in Figure 2.3 and listed below:

1. P_{20} ~ Maximum igniter pressure in the bed prior to propellant ignition
2. P_{21} ~ Pressure value in the bed prior to onset of propellant ignition
3. P_{2max} ~ Maximum combustion pressure in the bed
4. τ_{ign} ~ Ignition delay time from event initiation to onset of propellant combustion pressure rise

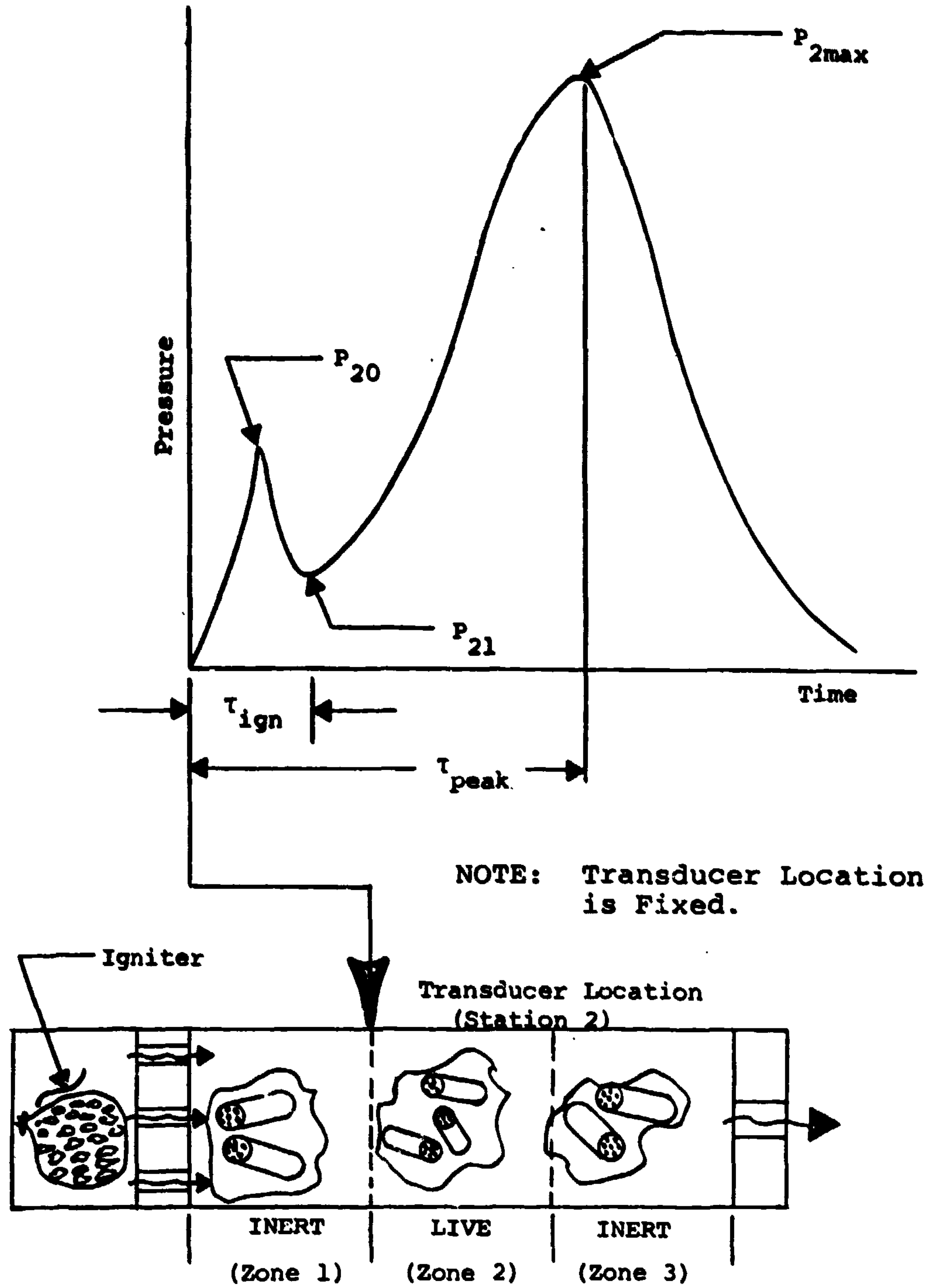

Figure 2.3 Pressure-time Nomenclature Assigned to IECD Data Reduction

5. τ_{peak} - Time from event initiation to peak combustion pressure

Oscilloscope data for all twenty-one (21) ignition effectiveness tests are presented in Appendix B.

Each Bruceton series conducted in Reference 1 and the current project, as shown in the experimental matrix, Table 2.5, was statistically reduced using a sensitivity method developed by Brownlee and Hodges (Reference 4) for small sample numbers to determine the 50 percent firepoint means (mass) presented in Table 2.6. Due to the limited number of shots in each Bruceton type series, the calculated means are subject to question; however, the calculated results are expected to be indicative of the relative ignition effectiveness of the igniter materials tested. Each of the mass means was multiplied by the experimentally determined heat of explosion to determine the 50 percent igniter energies presented in Table 2.7 and Figure 2.4. The data in Table 2.7 and Figure 2.4 indicate that the igniter energy requirements increase with increasing inert simulant bed thickness showing that the inert simulant zone is acting as an energy barrier, either by selectively blocking igniter materials and/or simply acting as an energy absorber during the inert heating phase. (This point is addressed more completely in the Data Analysis section).

2.3.2 Assessment of Data

A review of the NACO 50 percent firepoint data, Figure 2.4, suggests that the BP and $BKNO_3$ igniter streams are more effective than the MTV and the NC igniter materials. The general agreement of the NACO data for a bed length of 1.0 inch for all igniter materials suggests that the inert simulant zone is

Table 2.5 Ignition Effectiveness Experiments: Fifty Percent Firepoint Results

EXPERIMENTAL MATRIX

Propellant	Bed Length (in)	Igniter Material					
		BP	$BKNO_3$	NC	MTV	$BMoO_3$	AP
NACO	0.0						
	1.0	X	X	X		X	
	1.5	X	X	X	X	X	
	2.0	X	X	X	X		
LOVA	0.0	X	X	X	X	X	X
	1.0	X	X		X		
	1.5	X	X	X	X		X
	2.0						
NOSOL-318	0.0						
	1.0			X			
	1.5	X	X	X	X		
	2.0						
NOSOL-363	0.0						
	1.0						
	1.5	X	X	X	X		
	2.0						
PYRO	0.0						
	1.0						
	1.5			X			
	2.0						

Table 2.6 Ignition Effectiveness Experiments: Fifty Percent Firepoint Results

IGNITER CHARGE MASS (g)

Propellant	Bed Length (in)	Igniter Material					
		BP	$BKNO_3$	NC	MTV	$BMoO_3$	AP
NACO	0.0						
	1.0	1.27	0.67	1.10		3.64	
	1.5	1.65	0.90	2.38	1.10	5.75	
	2.0	2.78	1.07	2.85	1.54		
LOVA	0.0	2.77	1.58	3.50	1.72	NF	1.24
	1.0	4.03	2.07		1.94		
	1.5	5.75	2.55	4.30	2.95		2.59
	2.0						
NOSOL-318	0.0						
	1.0		1.90	1.31			
	1.5	4.40	1.80	3.05	1.63		
	2.0						
NOSOL-363	0.0						
	1.0						
	1.5	4.75	2.85	3.57	2.70		
	2.0						
PYRO	0.0						
	1.0						
	1.5			3.08			
	2.0						

NF - No Fire

Table 2.7 Ignition Effectiveness Experiments: Fifty Percent Firepoint Results

IGNITER CHARGE ENERGY (kcal)

Propellant	Bed Length (in)	Igniter Material					
		BP	$BKNO_3$	NC	MTV	$BMoO_3$	AP
NACO	0.0						
	1.0	0.9	1.0	1.0		0.9	
	1.5	1.2	1.4	2.2	1.7	1.4	
	2.0	2.0	1.6	2.6	2.4		
LOVA	0.0	2.0	2.4	3.2	2.6	NF	1.0
	1.0	2.9	3.1		3.0		
	1.5	4.1	3.8	4.0	4.5		2.1
	2.0						
NOSOL-318	0.0						
	1.0		2.8	1.2			
	1.5	3.1	2.7	2.8	2.5		
	2.0						
NOSOL-363	0.0						
	1.0						
	1.5	3.4	4.3	3.3	4.2		
	2.0						
PYRO	0.0						
	1.0						
	1.5			2.8			
	2.0						

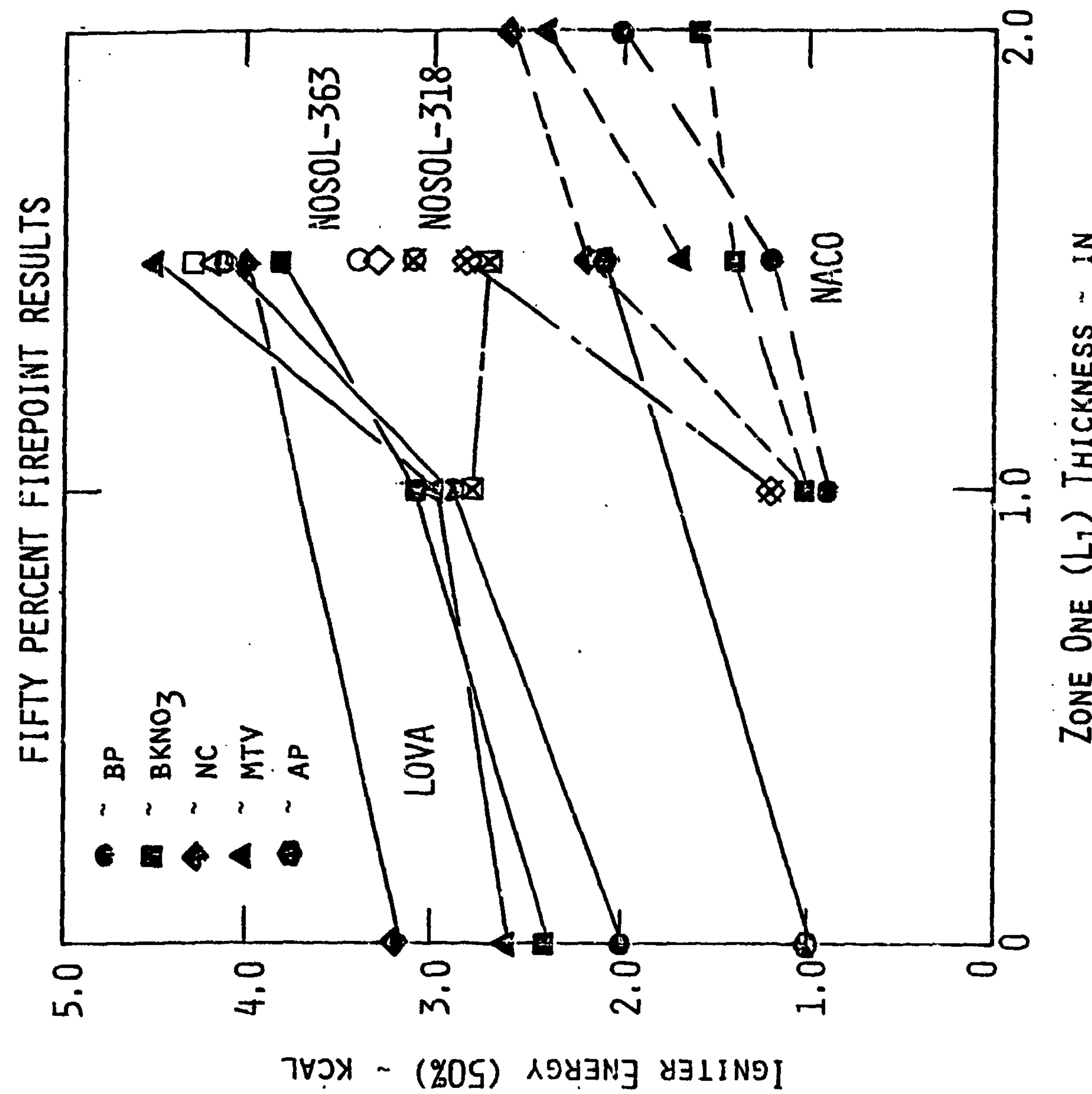

Figure 2.4 Fifty Percent Igniter Energy as a Function of Inert Bed Thickness

acting as a thermal sink and not very effective in selectively filtering the igniter products. This conclusion is based in part on the NC diagnostic tests where relatively poor igniter behavior was observed with unburned NC being a large fraction of the igniter "product" stream. If this line of thought is followed, the unburned NC contained in the igniter stream is effective in reaching the live propellant zone for an inert zone thickness of 1.0 inches, but is filtered out by the 1.5 inch and 2.0 inch inert zones, as indicated by the increase in ignition energy from 1.0 kcal to 2.2 kcal and 2.6 kcal, respectively. If this is correct, then an important conclusion can be reached with regard to the upstream energy transfer for the unburned NC igniter material. Specifically, if it is assumed that a portion of the NC is blocked by the inert zone and burns in the inert zone, then this energy liberation goes into heating the inert simulant and is not returned to the igniter gas stream in a time frame which can aid in the propellant ignition process. This observation tends to suggest that high solids igniter systems will be effective in stimulating a narrow zone adjacent to the vent location, but will be relatively poor in achieving a spatially in-depth ignition boundary.

NOSOL-318 ignition energy levels for an inert simulant zone thickness of 1.5 inches are relatively independent of igniter material type. The limited NOSOL-363 data indicate that BP and NC are more effective igniter materials than $BKNO_3$ and MTV. This observation suggests that the low gas content of the $BKNO_3$ and MTV products is contributing to a relatively large energy loss in the inert zone due to increased residence time (low transit velocity) for vapor and liquid phase transitions prior to entering the live propellant zone.

Ignition effectiveness data for LOVA propellants, Figure 2.4, generally indicate the low vulnerability aspects of the propellant system with significantly higher igniter energy levels required from all igniter materials tested, with the exception of the oxidizer rich products ammonium perchlorate igniter. Test data acquired for an inert simulant zone thickness of 0.0 inch (e.g., no inert simulant separating the igniter vents and the live propellant) exhibit ignition energy levels ranging from 2.0 kcal to 3.2 kcal for conventional igniter materials (BP, $BKNO_3$, NC, and MTV) and 1.0 kcal for the oxidizer rich AP igniter material. This observation suggests that the initial decomposition products of LOVA propellant are fuel rich, presumably in the gas phase, and are extremely reactive with the AP products.

Further support for the LOVA gas phase reaction step is indicated by the bed ignition pressure data presented in Table 2.8. Excluding the AP results for the moment, the lowest conventional igniter material energy level was for BP at a bed thickness of 0.0 inch and occurred at a bed pressure level of 1,300 psia. By contrast, the NC igniter system at $L_1 = 0.0$ inch required 3.2 kcal for LOVA ignition and occurred at a bed pressure level of 200 psia. In experiments which resulted in NO propellant ignition situations, no unburned igniter material was found in the housing or in the propellant bed (for tests conducted with $L_1 = 0.0$), except for the AP igniter system, and consequently, is presumed to have burned in the

Table 2.8 Ignition Effectiveness Experiments: Fifty Percent Firepoint Results

BED IGNITION PRESSURE ~ P_{20} (psia)

Propellant	Inert Bed Length (in)	BP	$BKNO_3$	NC	MTV	$BMoO_3$	AP
		Igniter Material					
NACO	0.0						
	1.0	500	200	30		30	
	1.5	300	100	100	200	100	
	2.0	700	200	200	300		
LOVA	0.0	1300	1000	200	900	NF	600
	1.0	1400	1100		600		
	1.5	2600	1400	3000	1000		900
	2.0						
NOSOL-318	0.0						
	1.0		700	80			
	1.5	1200	400	100	400		
	2.0						
NOSOL-363	0.0						
	1.0						
	1.5	1400	900	1800	700		
	2.0						
PYRO	0.0						
	1.0						
	1.5			100			
	2.0						

NOTE: P_{20} is measured at a fixed axial location with respect to the igniter vent exit; consequently, as the inert bed length varies, the bed ignition pressure location moves relative to the live propellant zone.

propellant region. Since the NC bed pressures were low relative to the BP bed pressures, it is presumed that the LOVA gas phase reaction did not contribute to the ignition energy balance, thus requiring a larger input from the NC igniter system. Another possibility is that the LOVA first step gas products are adversely affecting the NC product stream, thus inhibiting the NC/LOVA ignition sequence. It is interesting to note that the LOVA ignition energy levels correlate with the measured bed pressure levels, for conventional igniter materials, as shown in Table 2.9 below.

Table 2.9 LOVA Ignition Effectiveness at L_1 = 0.0 inch

Igniter	P_{20} Bed Pressure Level (psia)	Products Gas Phase Mass Fraction (%)	Fifty Percent Igniter Charge Energy (kcal)
AP	600	75.6	1.0
BP	1,300	54.8	2.0
$BKNO_3$	1,000	24.7	2.4
MTV	900	0.3	2.6
NC	200	90.8	3.2

The high theoretical products gas phase mass fraction for NC (90.8%) and the low bed pressure level is a further indication that the NC combustion is taking place in the bed and not in the igniter housing, or that the reaction is being inhibited by the LOVA products. Although $BKNO_3$ and MTV have relatively high mass fractions of product vapor and liquid phase materials (see Table 2.3), which should be more effective in the propellant inert heating and first decomposition step, the decreased igniter gas phase content apparently results in lower bed pressure levels and subsequent reduced reactivity of the LOVA decomposition.

In comparison, the AP igniter system produced 600 psi and required only 1.0 kcal for LOVA ignition. Ignition results for an inert bed thickness of 1.5 inches show the same relatively ignitibility difference between the conventional materials and the oxidizer rich AP igniter material, with energy levels of approximately 4 kcal being observed for conventional igniter materials as contrasted to 2.1 kcal for the AP igniter material.

3.0 DATA ANALYSIS

3.1 Qualitative Description of IECD Ignition Process

The IECD igniter venting process consists of an igniter jet which enters a finite thickness bed of inert simulant grains followed by a finite thickness bed of live propellant grains. The igniter jet is comprised of up to four different inert, or chemically active, stream types:

1. Hot gases,
2. Hot vapors capable of undergoing a phase change to either a liquid state or a solid state,
3. Hot liquids capable of undergoing a phase change to a solid state, and
4. Hot solids.

The manner in which the inert simulant bed affects each of these streams is speculation, but is postulated as follows. First, the inert simulant acts as a radiation buffer which is effective in reducing the igniter radiation incident upon the live propellant zone; consequently, the primary propellant ignition stimulus is presumed to be associated with the energy transported by the flowing igniter stream. Under this presumption, it then becomes important to establish the buffering effect of the inert simulant zone upon the multi-phase igniter stream as it flows from the igniter vent through the inert simulant. Since the inert simulant zone consists of a large number of randomly positioned pellets, it is reasonable to assume that the gas stream can pass through the inert bed relatively easily while experiencing a loss in both pressure and temperature prior to entering the live propellant zone, the losses being dependent upon the porosity and length of the inert simulant zone. Considering next the hot vapors, one can presume that the vapors can pass through the inert bed with the same relative ease as the hot gas stream; however, the pressure loss and temperature drop experienced by the gases and vapors would tend to drive the vapors toward a change in phase, with subsequent phase change energy release, presumably to a liquid which would be relatively effective in the inert heating phase of the live propellant ignition process. With regard to the hot liquids contained in the igniter stream, one can envision that the inert zone pellets may become wetted by the liquid stream during the flow process, thus reducing the initial liquid content potentially available for the live propellant zone. Of perhaps more significance is the possibility that the liquids initially present in the igniter products may undergo a phase change from liquid to solid within the confines of the inert zone, thus significantly reducing the potential effectiveness of the igniter stream to initiate combustion in the live propellant zone. Finally, if one applies the previous logic to the igniter solids flowing through the inert simulant bed, the higher trajectory momentum of the solids makes them less capable of traversing the inert zone without impacting the inert simulant pellets and becoming trapped in the inert zone, thus reducing the ignition potential of the igniter stream.

3.2 Analytical Procedures

The ignition effectiveness experiments presented in the previous section included data for zone one inert simulant bed thickness of 0.0, 1.0, 1.5, and 2.0 inches and presented 50 percent firepoint results based upon igniter energy levels (e.g., mass times HOE). Since the igniter energy level represents the maximum theoretical energy available to the packed bed system of inert simulant and live propellant, the 50 percent ignition energy levels previously presented need to be corrected to account for the energy losses experienced while flowing through the inert simulant bed. The analyses presented in this section provide a simplified approach for correcting the ignition energy levels for convective heat transfer losses while neglecting the perhaps more important effects of phase changes and particle entrapment.

Referring to Figure 3.1, the physical process is envisioned to consist of the following steps:

1. Igniter products are generated in the igniter housing at a pressure, $P_c(t)$, and a flame temperature, T_p. The assumption is made that the condensed phase products occupy negligible volume with respect to the gas phase.
2. Under the assumption of an ideal gas law and isentropic conditions, igniter products flow from the housing cavity via choked vents and expand supersonically to the bed free flow area (bore area minus blockage by pellets).
3. A strong normal shock is assumed to occur at the entrance to the packed bed, characterizing the subsonic flow field incident to the packed bed.
4. A spatially uniform flow field is assumed in the axial direction (e.g., no spatial gradients in pressure and temperature are considered.)

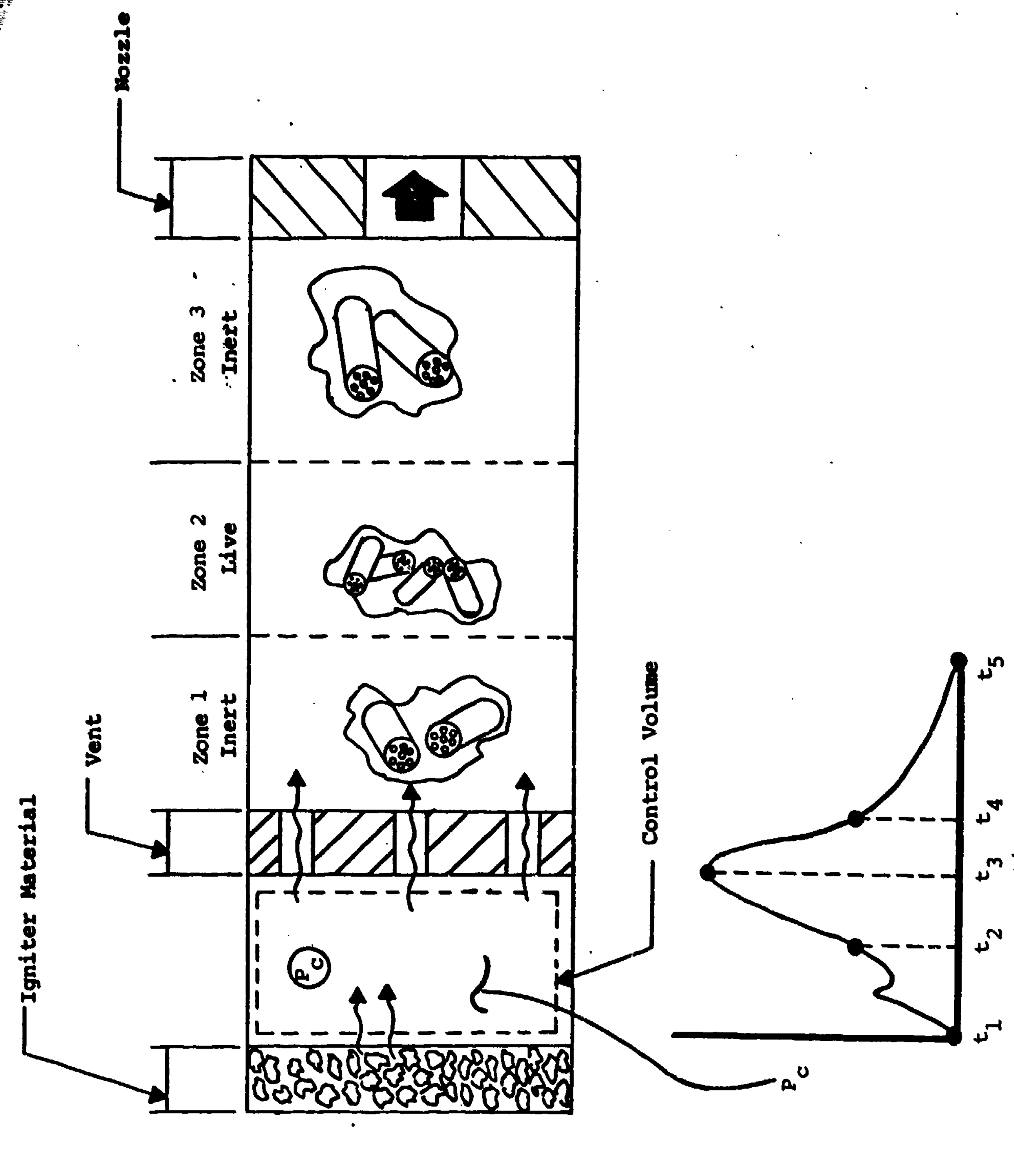

Figure 3.1 Schematic Representation of IECD Showing Igniter Control Volume

5. Bed convective heat losses are determined as a function of time in response to the experimentally measured igniter housing pressure-time curve, $P_c(t)$.

3.2.1 Igniter Mass Flux Characterization

Using the previous assumptions, the experimentally measured pressure-time curve, $P_c(t)$, is attributed to the gas phase products and may be used to calculate the igniter vent exit gas phase flow rate, $\dot{m}_g$

$$\dot{m}_g = \frac{D_e^* A_e P_c(t)}{\sqrt{\frac{R_g T_c}{\gamma g_c}}} \tag{1}$$

For sonic conditions, the compressible flow function, D_e^*, is given by

$$D_e^* = \left(\frac{\gamma+1}{2}\right)^{\frac{\gamma+1}{2(1-\gamma)}} \tag{2}$$

The mass of igniter products in the gas phase, m_g, is given by integrating the mass flux curve from the onset of ignition until expansion is complete.

$$m_g = \int_0^{\tau_{final}} \dot{m}_g dt \tag{3}$$

Substituting equations (1) and (2) into equation (3) under the assumption that the gas phase products temperature, T_c, is equal to the flame temperature, T_p, gives

$$m_g = \frac{D^* A_e}{\sqrt{\frac{R_g T_p}{\gamma g_c}}} \int_o^{\tau_{final}} P_c(t)dt \qquad (4)$$

The initial igniter mass, m_o, is known for each experiment; consequently, the condensed phase products mass, m_{cp}, is given by

$$m_{cp} = m_o - m_g - m_r - m_{ub} \qquad (5)$$

where m_o = initial charge mass
m_g = mass of gas phase products
m_r = post-test mass of residue remaining in igniter housing
m_{ub} = mass of unburned igniter material blown out of igniter vent into bed

In each test, the post-test residue mass was small for each igniter material; consequently, the pseudo-condensed phase mass (products plus unburned igniter material) can be determined from equation (5). Assume that the products condensed phase flow rate is proportional to the gas phase flow rate

$$\dot{m}_{cp} = \beta \dot{m}_g \qquad (6)$$

where β is defined by

$$\beta = \frac{m_{cp}}{m_g} \qquad (7)$$

Equations (4) and (5) provide two independent relations to solve for the three unknowns (m_g, m_{ub}, and β).

If the unburned solids were zero, then β would be uniquely determined by the pressure-time curve; however, since this is not the case for NC, a third relationship is required and will be provided by the energy balance equations.

3.2.2 Igniter Energy Characterization

The total exit energy flux, $\dot{E}_e$, will be considered to be comprised of the gas phase and the pseudo-condensed phase (products plus unburned) material streams

$$\dot{E}_e = \dot{E}_g + \dot{E}_{cp} \tag{8}$$

The gas phase energy flux, $\dot{E}_g$, is given by

$$\dot{E}_g = \dot{m}_g\left(C_{pg}T_e + \frac{V_e^2}{2}\right) \tag{9}$$

For sonic conditions at the vent exit, T_e and V_e may be expressed in terms of the chamber temperature, T_c to give

$$\dot{E}_g = \dot{m}_g\left[C_{pg}\left(\frac{2T_p}{\gamma+1}\right) + \frac{\gamma R_g T_p}{(\gamma+1)}\right] \tag{10}$$

where T_c has been assumed equal to T_p.

If one assumes no velocity lag between the gas phase and the condensed phase materials, the condensed phase energy flux is given by (approximately)

$$\dot{E}_{cp} \cong \dot{m}_{cp}\left(h_{cp} + \frac{V_e^2}{2}\right) + \dot{m}_{ub}\left(h_{ub} + \frac{V_e^2}{2}\right) \tag{11}$$

In the present analysis, the condensed phase products will be assumed to be at the gas phase flame temperature, T_p, and the unburned solids will be assumed to be at their original soak temperature, T_{so}. Since $\dot{m}_{cp}$ is a function of β, equation (11) may be rewritten as

$$\dot{E}_{cp} \cong \beta \dot{m}_g \left[C_{pcp} \left(\frac{2T_p}{\gamma+1} \right) + \frac{\gamma R_g T_p}{(\gamma+1)} \right] + \dot{m}_{ub} \left[C_{pub} T_{so} + \frac{\gamma R_g T_p}{(\gamma+1)} \right] \quad (12)$$

Closure of the balance equations and the proper solution for β is given by integrating the exit energy flux over the ballistic cycle to obtain the total energy leaving the vents

$$E_e = \int_o^{\tau_{final}} \dot{E}_e dt \quad (13)$$

The total energy calculated by equation (13) is compared to the theoretical igniter charge energy given by mass times HOE in an iterative fashion for β until a converged energy balance solution is achieved under the assumption that the unburned material flow rate is zero. If convergence is not achieved, then the unburned material flow rate is increased by a finite amount and the products condensed phase mass is reduced using equation (5) so that a mass balance is maintained. The final iterative solution provides the value of β that satisfies both the mass balance and energy balance equations simultaneously.

3.2.3 Bed Energy Loss Characterization

The igniter flow is assumed to expand from the vent orifice (throat) into the packed bed where a normal shock is formed, thus reducing the flow through the bed to subsonic conditions. Since the vent area is well specified and sonic throat conditions are assumed, the Mach number incident to the normal shock is determined by the area ratio for the vent flow expansion process. Define the bed porosity, ε_1, as

$$\varepsilon_1 = 1 - \frac{n_1 \bar{V}_{g1}}{\bar{V}_1} \tag{14}$$

where n_1 = number of grains in zone 1
$\bar{V}_{g1}$ = individual grain volume
$\bar{V}_1$ = bore volume of IECD in zone 1

If it is assumed that there is a large number of pellets per unit length of bed, then the expansion area ratio, (A/A*), is given by

$$\left(\frac{A}{A^*}\right)_1 = \frac{\varepsilon_1}{n_v}\left(\frac{D_1}{D_e}\right)^2 \tag{15}$$

where n_v = number of axial vents
D_e = vent diameter
D_1 = IECD bore diameter

The upstream incident Mach number is calculated from isentropic flow relations and is used with normal shock relations to fully specify the subsonic flow through the packed bed, including the following variables:

$M_1(t)$ ~ IECD in-bore Mach number
$P_1(t)$ ~ IECD in-bore static pressure
$T_1(t)$ ~ IECD in-bore static temperature
$\rho_1(t)$ ~ IECD in-bore static density
$V_1(t)$ ~ IECD in-bore velocity

With the gas dynamic variables determined as a function of time, the heat transfer to the packed bed can be calculated from the following Nusselt number correlation (Reference 5)

$$Nu_1 = 2 + 0.4\left(\frac{Re_1}{\varepsilon_1}\right)^{2/3} Pr^{1/3} \quad (16)$$

where

$$Nu_1 = \frac{h_{g1}D_{g1}}{k_{g1}}$$

The gas phase Reynolds number, Re_1, and thermal conductivity, k_{g1}, depend upon viscosity, μ, and Prandtl number, Pr, which are given by (Reference 6)

$$\mu_1 = 0.76 \times 10^{-3}\left(\frac{T_1}{537}\right)^{1.5} \Big/ (T_1 + 198) \quad (17)$$

and

$$Pr_1 = \frac{4\gamma}{(9\gamma-5)} \quad (18)$$

The local heat transfer rate to the grains, $\dot{Q}_1$, is given by

$$\dot{Q}_1 = h_{g1}*A_{s1}*(T_1(t) - T_s(t)) \quad (19)$$

where h_{g1} = gas phase heat transfer coefficient
A_{s1} = total grain heat transfer area
$T_s(t)$ = grain surface temperature

The gas phase heat transfer coefficient, h_{g1}, is obtained from the Nusselt number correlation given in equation (16)

$$h_{g1} = \frac{Nu_1*k_{g1}}{D_{g1}}$$

The single grain surface area is given by

$$A_{sg} = \frac{\pi}{2}\left(D_{g1}^2 - n_{p1}d_{p1}^2\right) + \pi D_{g1}L_{g1} + n_{p1}\pi d_{p1}L_{g1} \quad (20)$$

where n_{p1} = number of perforations
d_{p1} = perf diameter
D_{g1} = grain diameter
L_{g1} = grain length

The total grain heat transfer area, A_{s1}, is given by

$$A_{s1} = n_1 * A_{sg} \tag{21}$$

where n_1 is the total number of grains for each experiment.

The grain surface temperature, $T_s(t)$, is provided by one-dimensional, unsteady heating under the assumption that the grain thermal penetration zone is small in comparison to the propellant radius

$$\frac{T_s(t)-T_o}{T_1(t)-T_o} = 1 - \left[\exp \frac{h_{g1}{}^2 \alpha_s t}{k_s{}^2}\right] * \left[1 - \operatorname{erf}\left(\frac{h_{g1}\sqrt{\alpha_s t}}{k_s}\right)\right] \tag{22}$$

where α_s = grain thermal diffusivity
k_s = grain thermal conductivity
T_o = initial temperature

The heat transfer rate, $\dot{Q}_1$, may now be solved by equation (19) and integrated over the ballistic cycle to give the total heat transferred to the grains during the heating cycle, Q_1, shown in the following equation.

$$Q_1 = \int_0^{\tau_{final}} \dot{Q}_1 dt \qquad (23)$$

In a similar manner, the heat transfer loss from the stream to the wall, Q_{wl}, may be calculated by integrating

$$\dot{Q}_{wl} = \left(\frac{k_{gl}}{D_1}\right)\left[0.023\left(\frac{\mu_{gl}}{D_1 \rho_1 V_1}\right)^{0.2} Pr_1^{-2/3}\right] x$$

$$\left(T_1(t) - T_w\right) \qquad (24)$$

where T_w = IECD wall temperature (assumed constant)

The corrected energy incident to the live propellant in zone 2 is defined as E_{50} and is given by

$$E_{50} = E_e - Q_1 - Q_{wl} \qquad (25)$$

where E_e = total energy leaving igniter vents

Q_1 = total energy transferred to grains

Q_{wl} = total energy transferred to wall

These equations, although approximate in nature, will provide an order to magnitude assessment of the energy differential which exits between the igniter housing exit plane and the plane incident to the live propellant zone. Improvements in the procedure are warranted, particularly by including axial gradients in the packed bed and developing the effects of phase change and condensed phase trapping.

3.3 Data Analysis Results

The data analysis procedures presented in the previous section have been utilized to evaluate the igniter performance and to correct the 50 percent firepoint results for convective energy losses to the packed bed and IECD bore wall.

3.3.1 Igniter Calibration Data

Each igniter calibration pressure-time curve was tabulated into five pairs of pressure-time data, Table 3.1, and used as input conditions for the analysis model previously presented. Calculated gas phase mass fractions for the igniter product stream have been compared with theoretical values as determined by NASA-Lewis code computations (Table 2.3) and are presented in Table 3.2. Experimental values for BP are in reasonably good agreement with NASA-Lewis code values suggesting that the igniter behavior for the BP is reasonably good (Recall that the igniter system was originally designed for BP). Gas phase mass values for the four other igniter materials based upon integrated p-t data indicate that the gas production in the igniter cavity is low. This observation indicates that unburned igniter materials are contained in the vent exit streams. This conclusion is consistent with experimental observations for NC and AP tests; however, no unburned $BKNO_3$, or MTV, has ever been observed in the ignition effectiveness tests.

3.3.2 Corrected Zone Two Input Energy

Using the igniter calibration data previously presented in Table 3.1, bed and wall energy losses were determined as a function of igniter charge mass for each of the igniter materials used in the ignition

Table 3.1 Igniter Calibration Data

Test No.	Igniter Type	Igniter Mass (g)	t_1	P_1	t_2	P_2	t_3	P_3	t_4	P_4	t_5	P_5
			Time (ms)/Pressure (psia)									
I-001	BP	1.27	*									
-002	BP	1.27	0	0	.2	300	.25	900	.4	600	1.8	0
-003	BP	2.78	0	0	.5	1300	1.8	2300	4	1400	9	0
-004	BP	5.75	0	0	.6	3000	2.2	7500	4.2	2000	9	0
-005	BP	5.75	0	0	.6	3000	1.8	8000	4.0	1800	5.6	0
-006	BKN	0.90	0	0	.2	3000	.25	900	.4	800	2.1	0
-007	BKN	1.80	0	0	.4	1300	1.0	2100	3	1000	5.5	0
-008	BKN	2.85	0	0	.4	1300	1.1	2900	2.8	1000	4.7	0
-009	NC	1.10	0	0	.2	500	.25	900	.4	800	3.2	0
-010	NC	2.85	0	0	.2	700	.5	1400	1.5	600	2.6	0
-011	NC	4.30	0	0	1.0	2300	2.8	4400	4.6	2000	5.8	0
-012	MTV	1.10	0	0	.2	600	.3	1100	1.0	600	1.8	0
-013	MTV	1.94	0	0	.2	600	.25	1400	.7	500	1.3	0
-014	MTV	2.95	0	0	.2	600	.3	1500	1.6	500	2.3	0
-015	AP	1.24	0	0	.2	800	.3	1400	2.4	500	7	0
-016	AP	2.50	0	0	.2	800	.6	1800	1.6	1000	3.2	0

*No Scope Record

Table 3.2 Igniter Calibration Data

Product Mass Fraction: Gas Phase

Igniter Material	Mass (g)	Product Mass Fraction (Gas plus Vapor) Experimental*	NASA-Lewis
BP	1.27	.075	.558
	2.78	.590	.558
	5.75	.550	.558
$BKNO_3$	0.90	.132	.796
	1.80	.430	.796
	2.85	.289	.796
NC	1.10	.121	.902
	2.85	.061	.902
	4.30	.330	.902
MTV	1.10	.125	.399
	1.94	.049	.399
	2.95	.078	.399
AP	1.24	.374	.756
	2.50	.156	.756

*Experimental calculations based upon one shot each.

effectiveness tests. The calculated energy losses were then subtracted from the igniter total energy to give a corrected zone two input energy as a function of igniter mass. These results, presented in Appendix C for BP, $BKNO_3$, NC, MTV, and AP permit the graphical determination of corrected energy levels for 50 percent igniter mass test values which lie between the three igniter calibration charge masses.

Using the experimentally determined 50 percent firing point mass quantities previously presented in Table 2.6, corrected zone two input energies have been determined for all ignition effectiveness experiments and are presented in Table 3.3. Corrected zone two input energies for NACO and LOVA propellants, respectively, are presented in Figures 3.2 and 3.3 for BP, $BKNO_3$, NC, MTV, and AP igniter materials as a function of zone one inert bed length (L_1). If the process for determining the bed energy losses were correct (including thermophysical properties), one would expect the corrected energy levels to have a zero slope with zone one thickness changes. The NACO data for BP and $BKNO_3$, Figure 3.2, exhibit this general trend and suggest that the 50 percent firepoint for NACO is about 1.0 kcal. The NACO results for NC and MTV both appear to agree with the 1.0 kcal ignition energy value at L_1 = 1.0 inch, but both exhibit increasing ignition energy requirements with increasing zone one length. Since BP igniter material exhibited high products gas phase mass fractions and the energy correction procedures are based on gas phase convection heat transfer, the NC and MTV trends tend to suggest that other heat loss mechanisms are dominant.

The LOVA results presented in Figure 3.3 for conventional igniter materials indicate that the

Table 3.3 Ignition Effectiveness Experiments:
Fifty Percent Firepoint Results

Corrected Zone Two Input Energy (kcal)

Propellant	Bed Length (in)	Igniter Material: BP	$BKNO_3$	NC	MTV	$BMoO_3$	AP
NACO	0.0						
	1.0	0.9	1.0	0.9		-	
	1.5	0.8	1.2	2.1	1.6	-	
	2.0	0.8	1.3	2.4	2.2		
LOVA	0.0	2.0	2.4	3.2	2.6		1.0
	1.0	2.2	2.7		3.0		
	1.5	3.0	3.2	3.3	4.3		2.0
	2.0						
NOSOL-318	0.0						
	1.0		2.5	1.2			
	1.5	2.1	2.2	2.6	2.4		
	2.0						
NOSOL-363	0.0						
	1.0						
	1.5	2.3	3.8	3.0	4.0		
	2.0						
PYRO	0.0						
	1.0						
	1.5			2.6			
	2.0						

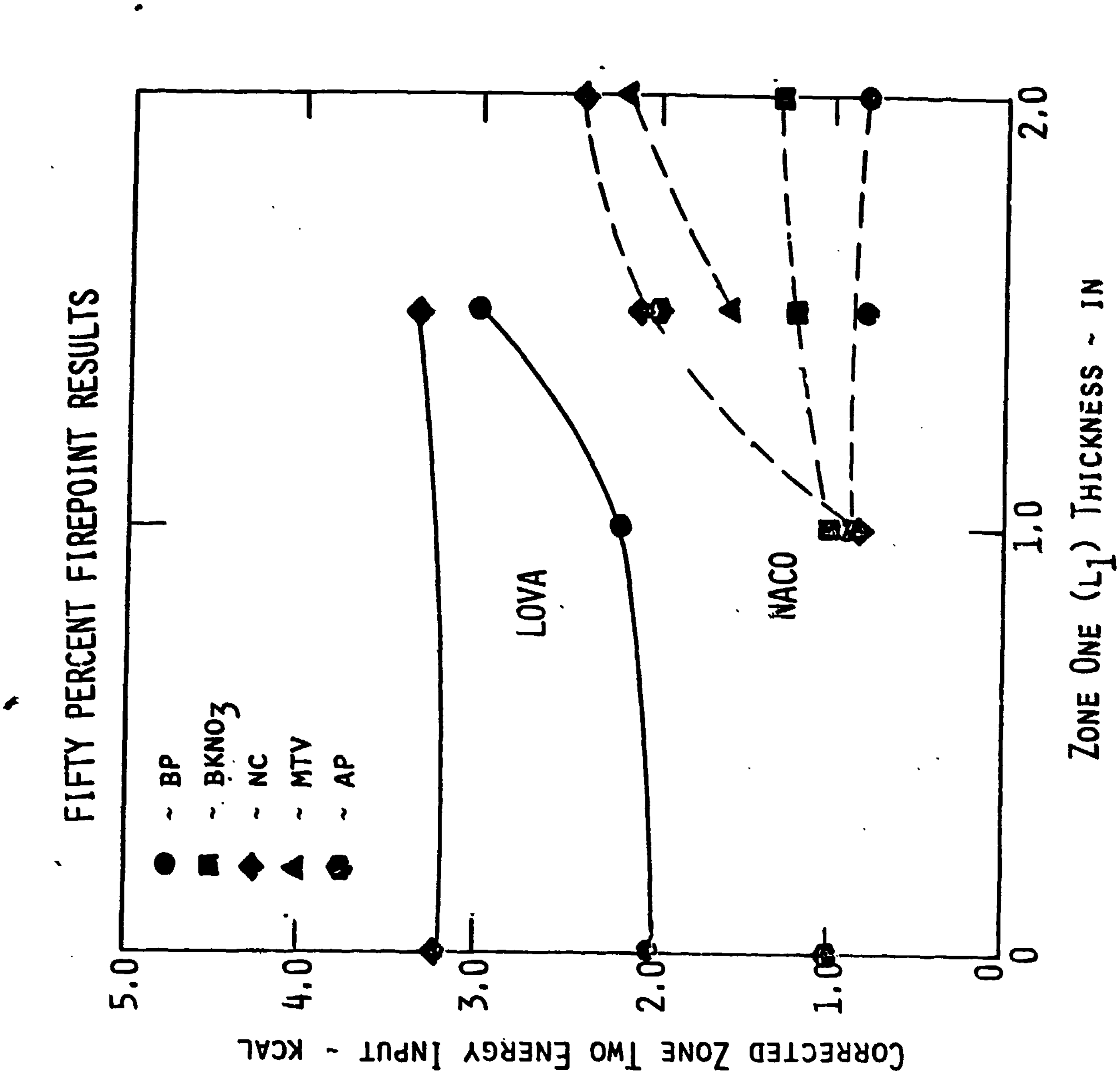

Figure 3.2 Corrected Zone Two Input Energies for NACO Propellant as a Function of Inert Bed Length

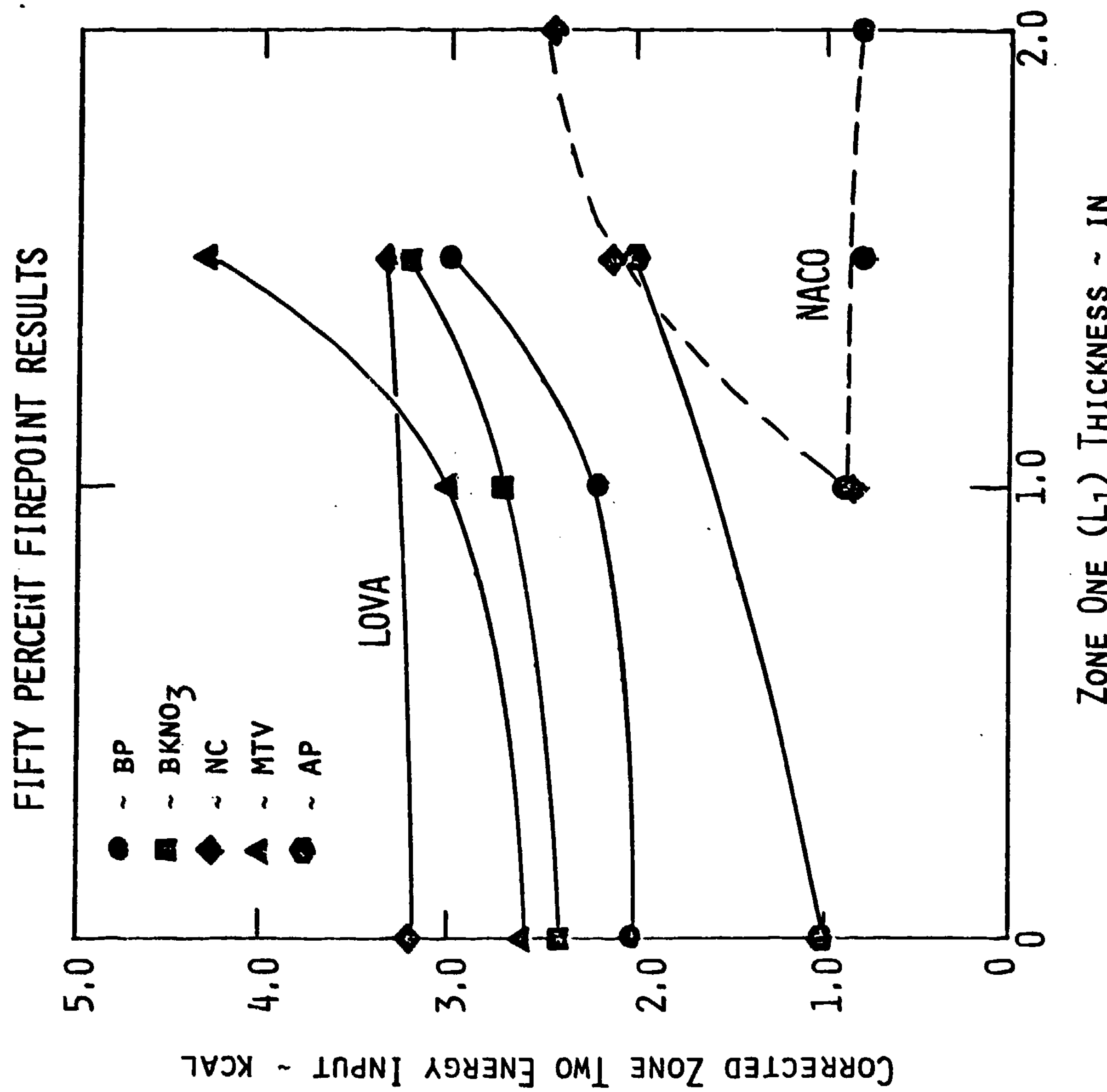

Figure 3.3 Corrected Zone Two Input Energies for LOVA Propellant as a Function of Inert Bed Length

ignition energy requirements for LOVA are approximately twice as great as the NACO requirements. By contrast, the oxidizer rich AP igniter data indicate that the ignitibility boundary of LOVA propellant can be significantly reduced by the presence of oxidizer rich species in the igniter stream. The LOVA data for BP, $BKNO_3$, and MTV show a slightly increasing slope for bed thicknesses up to 1.0 inch with a noticeable slope increase from 1.0 inch to 1.5 inches. These results indicate that the convective energy correction procedures previously developed are not adequate for LOVA propellant.

Corrected zone two input energies for NACO and LOVA propellants are presented in Figure 3.4 for BP, $BKNO_3$, NC, MTV, and AP igniter materials as a function of theoretical flame temperature (T_p) at 500 psia. NACO data are shown for inert bed lengths of 1.5 inches and 2.0 inches and show no definitive energy minimum correlation with flame temperature. In fact, low ignition energy levels of 1 kcal were observed for BP (1930°K) and $BKNO_3$ (2890°K), whereas high ignition energy levels of 2 kcal were observed for NC (2350°K) and MTV (2650°K). The LOVA results exhibited the same general trends for conventional igniter materials and a low ignition energy level of 1 kcal for AP (1400°K).

Additional corrected zone two energy input correlations are shown in Figures 3.5-3.8 for NACO and LOVA propellants as a function of the igniter products mass fraction. Figures 3.5 and 3.6 present the corrected zone two input energy for NACO and LOVA propellants, respectively, as a function of the liquid phase mass fraction where it can be seen that ignition energy requirements decrease as the liquid phase mass fraction

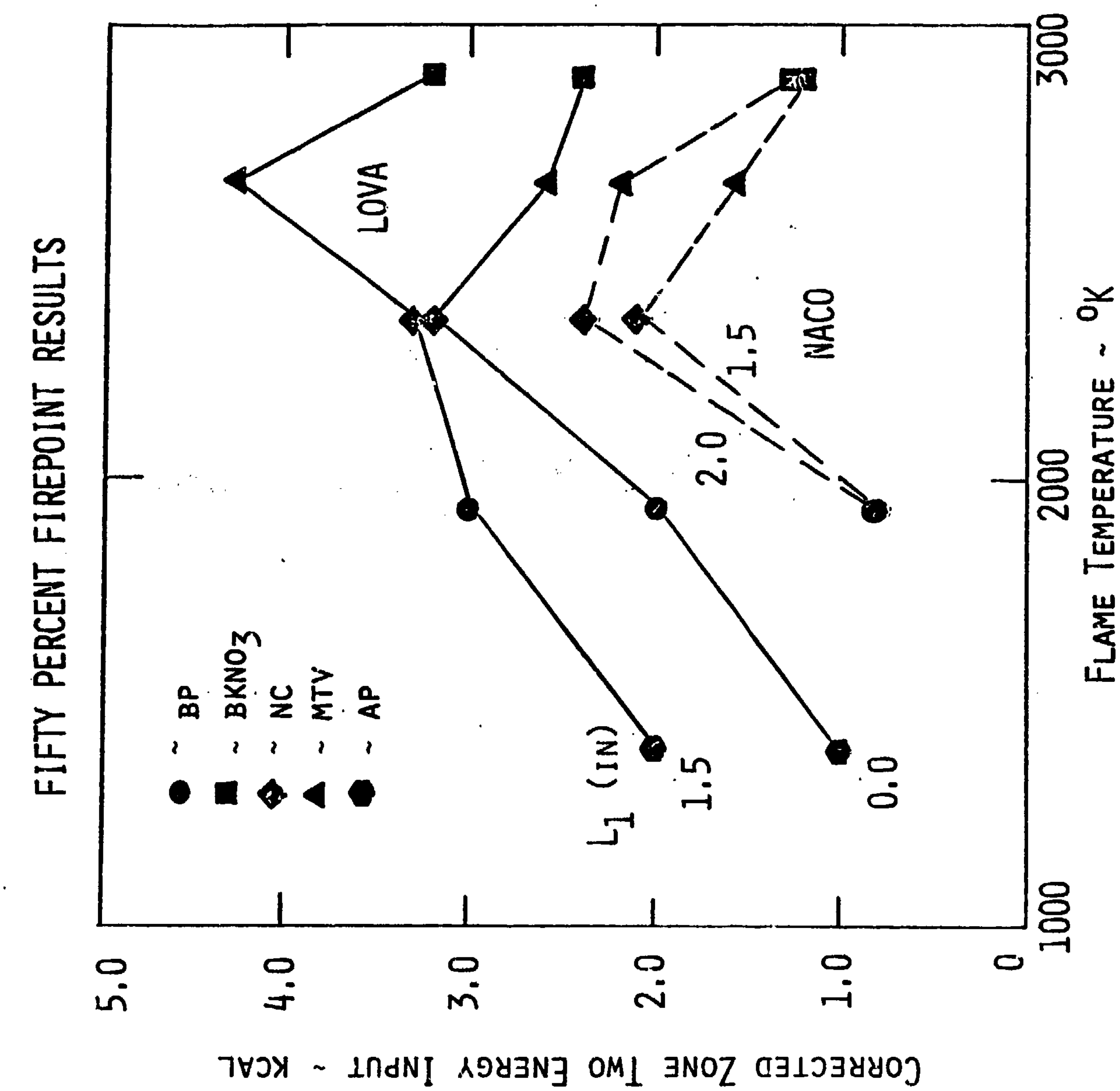

Figure 3.4 Corrected Zone Two Input Energies for LOVA and NACO Propellant as a Function of Igniter Material Flame Temperature

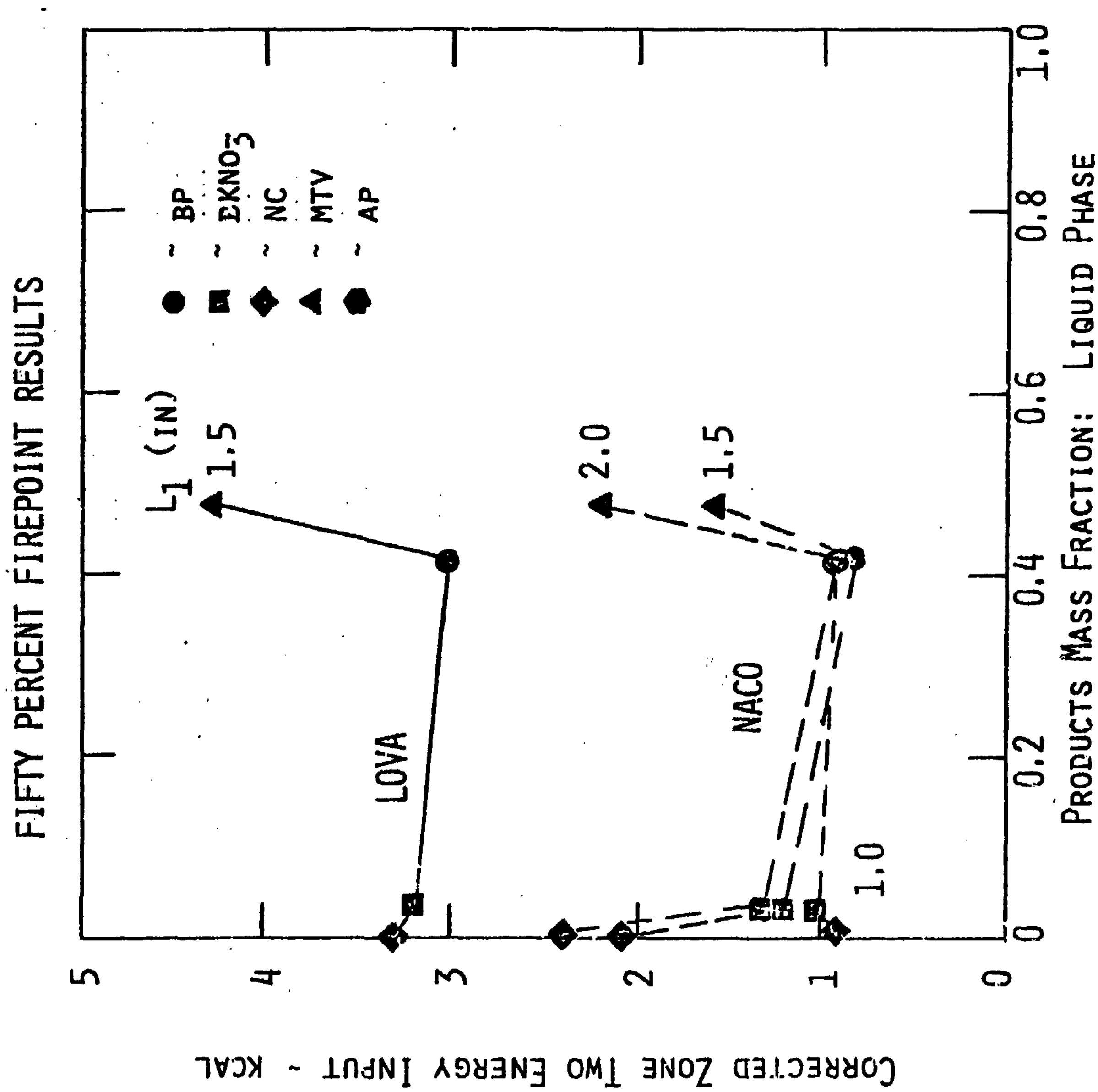

Figure 3.5 Corrected Zone Two Input Energies for NACO Propellant as a Function of Liquid Phase Mass Fraction

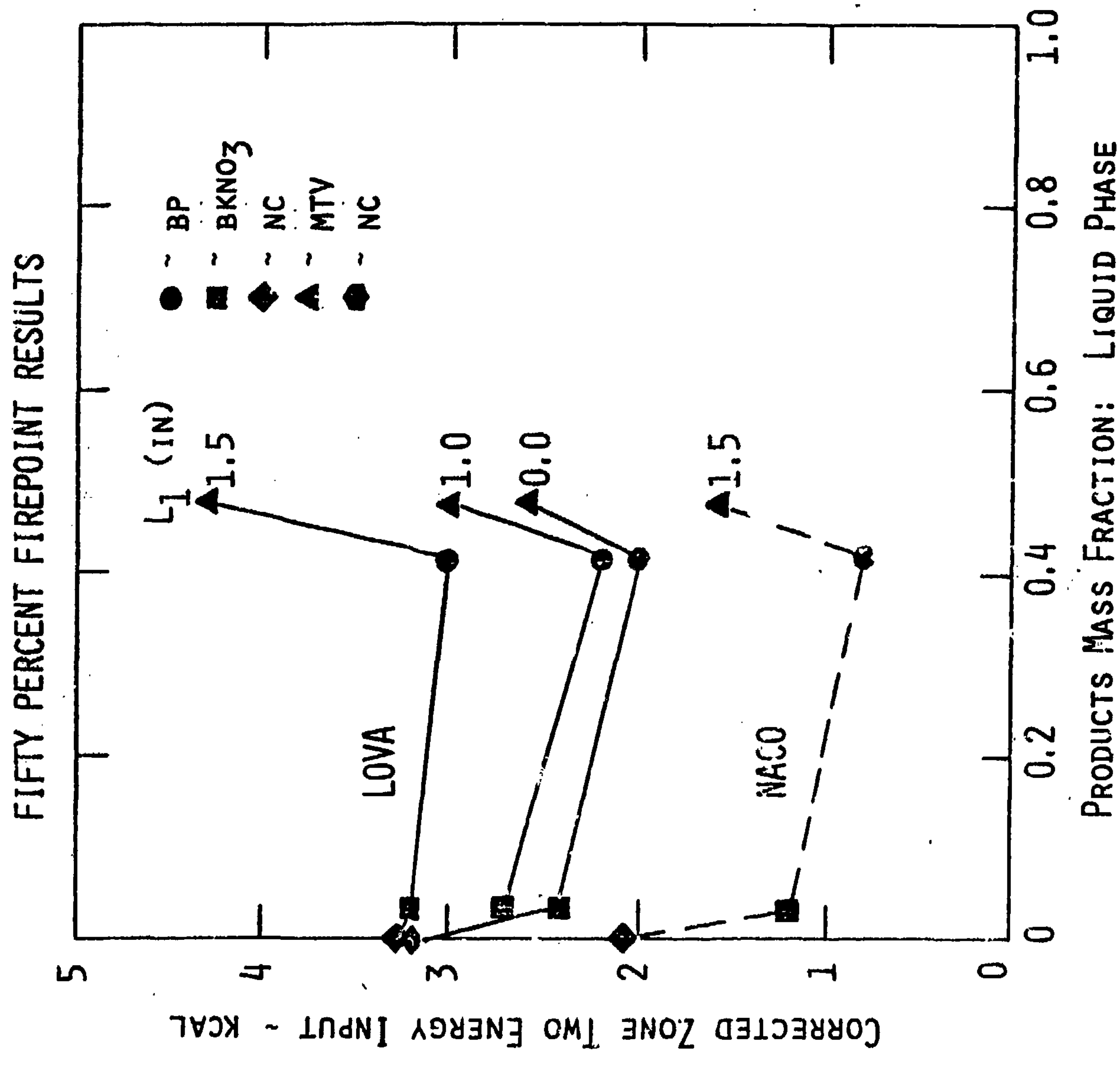

Figure 3.6 Corrected Zone Two Input Energies for LOVA Propellant as a Function of Liquid Phase Mass Fraction

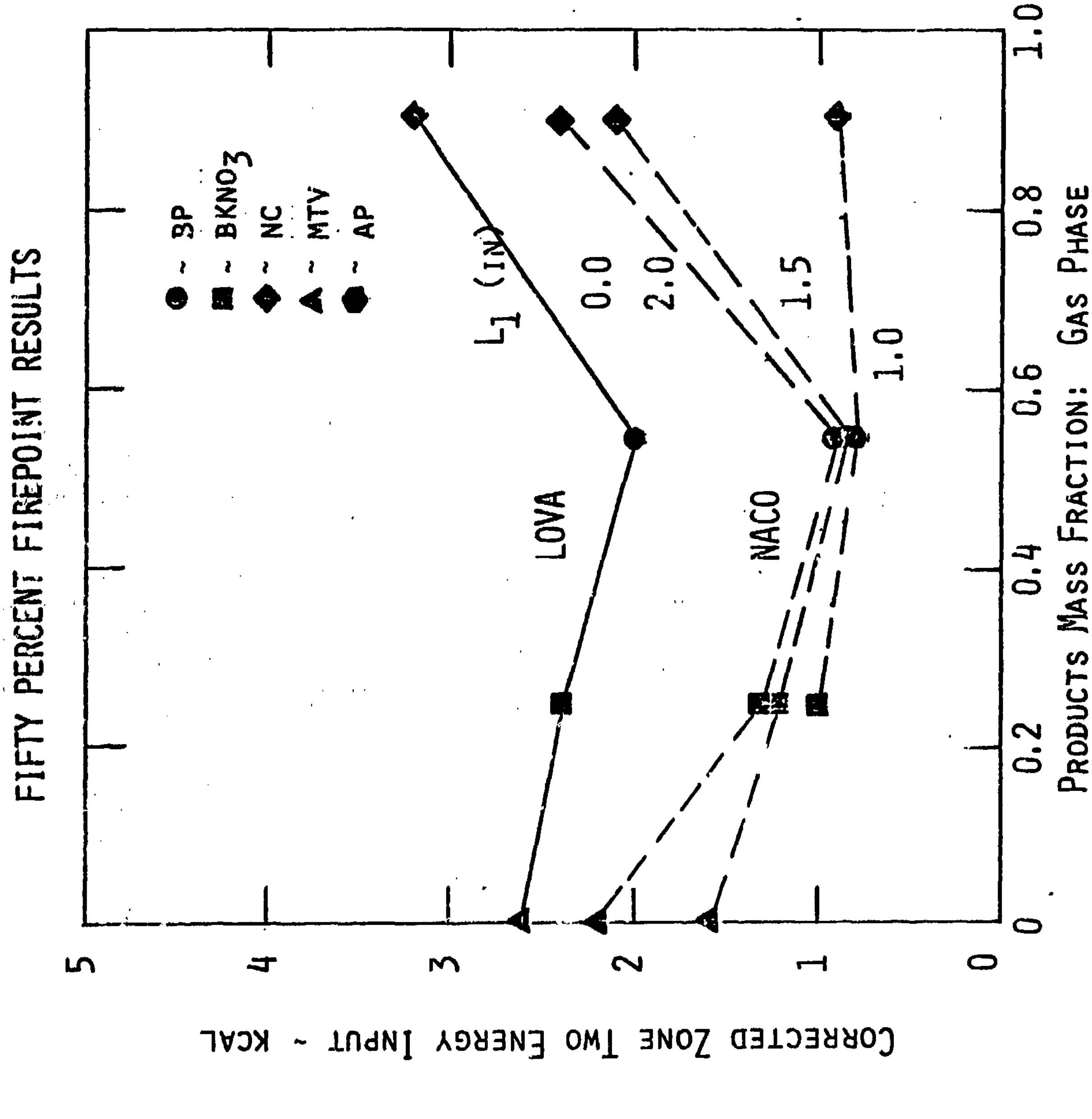

Figure 3.7 Corrected Zone Two Input Energies for NACO Propellant as a Function of Gas Phase Mass Fraction

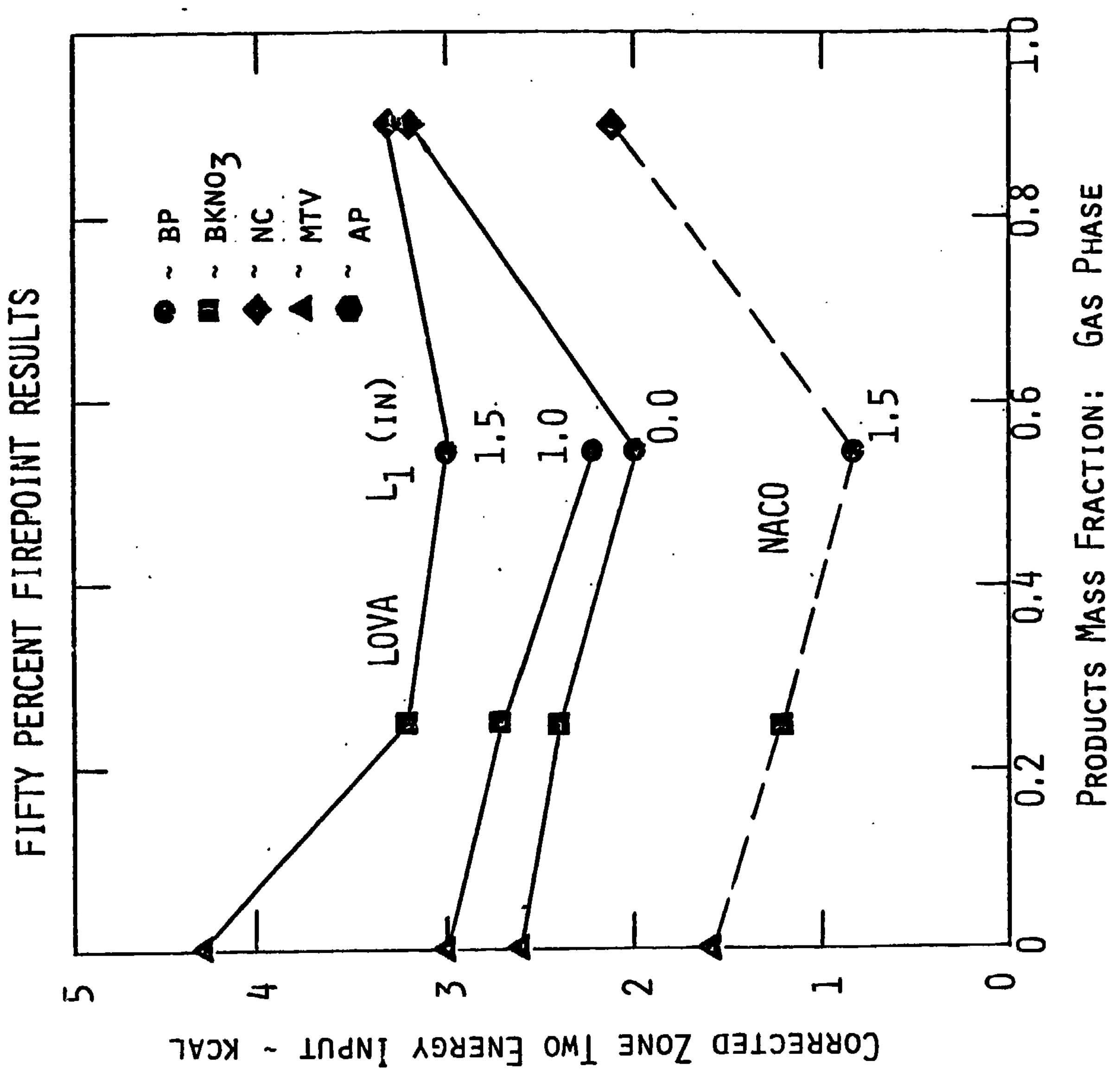

Figure 3.8 Corrected Zone Two Input Energies for LOVA Propellant as a Function of Gas Phase Mass Fraction

increases from 0.0 (NC) to about 0.4 (BP), followed by a sharp increase at a mass fraction of 0.48 (MTV). This trend suggests that liquid phase products are beneficial, but that something present in the BP stream is absent in the MTV igniter stream. Figures 3.7 and 3.8 present the corrected zone two input energy for NACO and LOVA propellants, respectively, as a function of gas phase mass fraction where an ignition energy minimum is observed at a gas phase mass fraction of 0.5 (BP). Both MTV (0.3% gas) and NC (91% gas) exhibit two-fold increases in ignition energy requirements relative to BP. These results suggest that the establishment of a gas phase convective flow field is necessary to the propellant ignition process. Since BP and MTV both have comparable liquid phase mass fractions, which should favor propellant heating (particularly for the higher temperature MTV liquid), the increased performance of the BP igniter system appears to be a result of the gas phase's ability to convectively drive the liquid phase through the propellant bed. By referring to Figures 3.5 and 3.6, one could speculate that if MTV had a higher gas phase mass fraction (say 25% to 50% gas), the ignition energy requirements for MTV would be greatly reduced. On the other hand, the NC results suggest that an all gas chemically inert igniter will perform as poorly as a system with a low gas mass fraction (MTV). Figures 3.5-3.8 suggest that the optimum igniter product stream would consist of 30-50% in the gas phase and 30-50% in the liquid phase. It is felt that the 30-50% liquid phase mass fraction could be partitioned between the solid phase and the liquid phase depending upon the ignition boundary pattern desired in the propellant bed. That is, if a higher solids mass fraction were present, the propellant would trap the hot particles and propellant ignition would occur locally near the vents. On the other hand, if a higher liquid mass fraction were used, the igniter vent jet would penetrate the propellant bed more completely and a more distributed propellant ignition boundary would be formed.

3.4 Some Qualitative Observations

Although the major focus of the project was placed upon determining fifty percent firepoint ignition energy levels, several general observations were made during the experimental portions of the project, especially for NO-fire situations, and will be presented in this section.

In experiments conducted with NACO propellant, propellant ignition was easy to achieve for relatively low igniter energy levels with all igniter materials tested. In each Bruceton series, the tests usually consisted of 5-6 YES-fires and 5-6 NO-fires and, in all cases, the post-test NO-fire propellant was closely examined. In general, the NACO propellant surface showed evidence of a melt layer forming with the presence of craters randomly located on the surface. In general, post-test propellant weighings indicated a five percent mass loss had occurred. In most NO-fire experiments with BP, $BKNO_3$, and MTV, the NACO propellant grains were fused together by the frozen melt layer. This situation was never observed in the NC experiments (although the melt layer was observed), presumably because the igniter pressure pulse was too low in magnitude or of insufficient duration to promote the fusing action. The implication of these observations is that perhaps the propellant form function during the early stages of burning bears no resemblance at all to the packed bed grain geometry, and in actuality, much less area is available for surface burning in the propellant ignition phase than codes would predict as necessary for proper ignition transfer.

In experiments conducted with LOVA propellant, initial tests were conducted with the same igniter configuration as was utilized with NACO, NOSOL-363, and NOSOL-318 propellants without achieving any propellant ignitions (e.g., no bed pressure rise other than the igniter input pulse) even though LOVA propellant mass loss as great as fifty percent of the original mass had taken place. Initial speculation was that the igniter jet axial velocity was too high to permit ample residence time for the LOVA first step decomposition products to fully react (with sufficient exothermic heat release) to initiate propellant combustion. Igniter vent changes to larger vents (e.g., reduced vent axial velocity) improved the situation slightly, but no prompt LOVA ignitions were achieved and LOVA "erosive" mass loss was approaching 75 percent of the original charge. In order to provide greater residence time between the igniter products and the LOVA products, the bed axial flow velocity was lowered by reducing the IECD aft closure bleed orifice by 40 percent. When this change was made, prompt ignitions were achieved. These observations suggest that there exists a gas phase ignition step which is rather slow and requires a reaction time on the order of the flow transit time. These tests, in conclusion, show that it was reasonable to assume that the LOVA gas phase decomposition products would be fuel rich and, consequently, the reaction could be accelerated by the presence of oxidizer species in the igniter stream. Subsequent tests were conducted with an oxidizer rich igniter (100% AP) and LOVA ignition energy requirements were reduced 2-3 times relative to firings conducted with conventional igniter materials. Although these firings are not conclusive, there is strong evidence to suggest the presence of an active, fuel rich LOVA gas phase decomposition step.

4.0 REFERENCES

1. Varney, A. Michael and Martino, John, "Expanded Ignition Effectiveness Tests of Selected Igniter Materials with Navy Propellants," Final Technical Report on Contract N00174-81-C-0453, ACT-TR-8136, Applied Combustion Technology, Inc., Orlando, FL, August 1982.
2. Varney, A. Michael, Martino, John, and Henry, Rod, "Ignition Effectiveness Tests of Selected Igniter Materials with Navy Gun Propellants," 19th JANNAF Combustion Meeting, Greenbelt, MD, October 1982.
3. Varney, M., Keeser, J., and Brandstadt, R., "An Ignition Energetics Characterization Device for Porous Bed Gun Propellants," 16th JANNAF Combustion Meeting, Monterey, CA, September 1979.
4. Brownlee, K. A., Hodges, J. L., and Rosenblatt, M., "The Up-and-Down Method with Small Samples," J. of America Statistical Association, Volume 48, 1953.
5. Gelperin, N. and Einstein, V., "Heat Transfer in Fluidized Beds," Fluidization, Academic Press, 1971.
6. Gough, P. S., "Numerical Analysis of a Two-Phase Flow with Explicit Internal Boundaries," IHCR-77-5, Naval Ordnance Station, Indian Head, MD, 1977.

APPENDIX A

Ignition Effectiveness Test

IECD Run Log

Bed Length (in)	Propellant	Igniter Material	Page No.
0.0	LOVA	BP	A-1
	LOVA	$BKNO_3$	A-2
	LOVA	MTV	A-3
	LOVA	NC	A-4
	LOVA	AP	A-5
1.0	NACO	BP	A-6
	NACO	$BKNO_3$	A-7
	NACO	NC	A-8
	NACO	$BMoO_3$	A-9
	N318	$BKNO_3$	A-10
	N318	NC	A-11
	LOVA	BP	A-12
	LOVA	$BKNO_3$	A-13
	LOVA	$BMoO_3$	A-14
	LOVA	MTV	A-15
1.5	NACO	BP	A-16
	NACO	$BKNO_3$	A-17
	NACO	NC	A-18
	NACO	MTV	A-19
	NACO	$BMoO_3$	A-20
	N318	BP	A-21
	N318	$BKNO_3$	A-22
	N318	NC	A-23
	N318	MTV	A-24
	N363	BP	A-25
	N363	$BKNO_3$	A-26
	N363	NC	A-27
	N363	MTV	A-28
	LOVA	$BKNO_3$	A-29 & 30
	LOVA	BP	A-31
	LOVA	MTV	A-32
	LOVA	NC	A-33
	PYRO	NC	A-34
	LOVA	AP	A-35
2.0	NACO	BP	A-36
	NACO	$BKNO_3$	A-37
	NACO	NC	A-38
	NACO	MTV	A-39

IECD IGNITION EFFECTIVENESS TEST DATA

(Inert Simulant Zone 1 Thickness 0.00 in)

	Igniter				Propellant		
Test Number	Configuration	Matl	Mass (g)	δm (g)	Matl	Mass (g)	Ignition (yes/no)
4001	4080AV	BP	0.0	.5	LOVA	40	No
4002	4080AV	BP	0.0	.5	LOVA	40	No
4003	4080AV	BP	1.0	.5	LOVA	40	No
4004	4080AV	BP	1.5	.5	LOVA	40	No
4005	4080AV	BP	2.0	.5	LOVA	40	No
4006	5113	BP	2.0	.5	LOVA	40	No
4007	5113	BP	3.0	.5	LOVA	40	No
4008	5113	BP	4.0	.5	LOVA	40	Yes
4009	5113	BP	3.5	.5	LOVA	40	Yes
4010	5113	BP	3.0	.5	LOVA	40	Yes
4011	5113	BP	2.5	.5	LOVA	40	No
4012	5113	BP	3.0	.5	LOVA	40	Yes
4013	5113	BP	2.5	.3	LOVA	40	No
4014	5113	BP	2.8	.3	LOVA	40	Yes
4015	5113	BP	2.5	.3	LOVA	40	Yes
4016	5113	BP	2.2	.3	LOVA	40	No
4017	5113	BP	2.5	.3	LOVA	40	No
4018	5113	BP	2.8	.3	LOVA	40	No
4019	5113	BP	3.1	.3	LOVA	40	Yes
4020	5113	BP	2.8	.3	LOVA	40	No
4021	5113	BP	3.1	.3	LOVA	40	Yes
4022	5113	BP	2.8	.3	LOVA	40	No
4023	5113	BP	3.1	.3	LOVA	40	Yes

IECD IGNITION EFFECTIVENESS TEST DATA

(Inert Simulant Zone 1 Thickness 0.00 in)

Test Number	Igniter Configuration	Igniter Matl	Igniter Mass (g)	Igniter δm (g)	Propellant Matl	Propellant Mass (g)	Ignition (yes/no)
4024	5113	BKN	1.4	.3	LOVA	40	No
4025	5113	BKN	1.7	.3	LOVA	40	Yes
4026	5113	BKN	1.4	.3	LOVA	40	No
4027	5113	BKN	1.7	.3	LOVA	40	Yes
4028	5113	BKN	1.4	.2	LOVA	40	No
4029	5113	BKN	1.6	.2	LOVA	40	No
4030	5113	BKN	1.8	.2	LOVA	40	Yes
4031	5113	BKN	1.6	.2	LOVA	40	Yes
4032	5113	BKN	1.4	.2	LOVA	40	No
4033	5113	BKN	1.6	.2	LOVA	40	Yes
4034	5113	BKN	1.4	.2	LOVA	40	No
4035	5113	BKN	1.6	.2	LOVA	40	No
4036	5113	BKN	1.8	.2	LOVA	40	Yes
4037	5113	BKN	1.6	.2	LOVA	40	Yes
4038	5113	BKN	1.4	.2	LOVA	40	No

IECD IGNITION EFFECTIVENESS TEST DATA

(Inert Simulant Zone 1 Thickness 0.00 in)

	Igniter				Propellant		
Test Number	Configuration	Matl	Mass (g)	δm (g)	Matl	Mass (g)	Ignition (yes/no)
4039	5113	MTV	1.5	.3	LOVA	40	No
4040	5113	MTV	1.8	.3	LOVA	40	Yes
4041	5113	MTV	1.5	.3	LOVA	40	No
4042	5113	MTV	1.8	.3	LOVA	40	Yes
4043	5113	MTV	1.7	.2	LOVA	40	No
4044	5113	MTV	1.9	.2	LOVA	40	Yes
4045	5113	MTV	1.7	.2	LOVA	40	No
4046	5113	MTV	1.9	.2	LOVA	40	Yes
4047	5113	MTV	1.7	.2	LOVA	40	Yes
4048	5113	MTV	1.5	.2	LOVA	40	No
4049	5113	MTV	1.7	.2	LOVA	40	Yes
4050	5113	MTV	1.5	.2	LOVA	40	No
4051	5113	MTV	1.7	.2	LOVA	40	No
4052	5113	MTV	1.9	.2	LOVA	40	Yes
4053	5113	MTV	1.7	.2	LOVA	40	Yes

IECD IGNITION EFFECTIVENESS TEST DATA

(Inert Simulant Zone 1 Thickness 0.00 in)

	Igniter				Propellant		
Test Number	Configuration	Matl	Mass (g)	δm (g)	Matl	Mass (g)	Ignition (yes/no)
4054	5113	NC	2.2	.5	LOVA	40	No
4055	5113	NC	2.7	.5	LOVA	40	No
4056	5113	NC	3.2	.5	LOVA	40	No
4057	5113	NC	3.7	.5	LOVA	40	Yes
4058	5113	NC	3.2	.5	LOVA	40	No
4059	5113	NC	3.7	.4	LOVA	40	Yes
4060	5113	NC	3.3	.4	LOVA	40	Yes
4061	5113	NC	2.9	.4	LOVA	40	No
4062	5113	NC	3.3	.4	LOVA	40	No
4063	5113	NC	3.7	.4	LOVA	40	Yes
4064	5113	NC	3.3	.4	LOVA	40	No
4065	5113	NC	3.7	.4	LOVA	40	Yes
4066	5113	NC	3.3	.4	LOVA	40	No
4067	5113	NC	3.7	.4	LOVA	40	No
4068	5113	NC	4.1	.4	LOVA	40	Yes
4069	5113	NC	3.7	.4	LOVA	40	Yes

IECD IGNITION EFFECTIVENESS TEST DATA

(Inert Simulant Zone 1 Thickness 0.00 in)

	Igniter				Propellant		
Test Number	Configuration	Matl	Mass (g)	δm (g)	Matl	Mass (g)	Ignition (yes/no)
4133	5113	AP	2.0	1.0	LOVA	40	Yes
4134	5113	AP	1.0	.5	LOVA	40	No
4135	5113	AP	1.5	.2	LOVA	40	Yes
4136	5113	AP	1.3	.2	LOVA	40	Yes
4137	5113	AP	1.1	.2	LOVA	40	No
4138	5113	AP	1.3	.2	LOVA	40	Yes
4139	5113	AP	1.1	.2	LOVA	40	No
4140	5113	AP	1.3	.2	LOVA	40	Yes
4141	5113	AP	1.1	.2	LOVA	40	No
4142	5113	AP	1.3	.2	LOVA	40	No
4143	5113	AP	1.5	.2	LOVA	40	Yes
4144	5113	AP	1.3	.2	LOVA	40	Yes
4145	5113	AP	1.1	.2	LOVA	40	No
4146	5113	AP	1.3	.2	LOVA	40	Yes

IECD IGNITION EFFECTIVENESS TEST DATA

(Inert Simulant Zone 1 Thickness 1.00 in)

		Igniter			Propellant		
Test Number	Configuration	Matl	Mass (g)	δm (g)	Matl	Mass (g)	Ignition (yes/no)
173	4080AV	PRIMER ONLY			NACO	40	No
174	4080AV	BP	1.0	.3	NACO	40	Yes
175	4080AV	BP	.7	.3	NACO	40	No
176	4080AV	BP	1.0	.3	NACO	40	No
177	4080AV	BP	1.3	.3	NACO	40	No
178	4080AV	BP	1.6	.3	NACO	40	Yes
179	4080AV	BP	1.3	.3	NACO	40	No
180	4080AV	BP	1.6	.3	NACO	40	Yes
181	4080AV	BP	1.3	.3	NACO	40	Yes
182	4080AV	BP	1.0	.3	NACO	40	No
183	4080AV	BP	1.3	.3	NACO	40	Yes
184	4080AV	BP	1.0	.3	NACO	40	No
185	4080AV	BP	1.3	.3	NACO	40	Yes

IECD IGNITION EFFECTIVENESS TEST DATA

(Inert Simulant Zone 1 Thickness 1.00 in)

	Igniter				Propellant		
Test Number	Configuration	Matl	Mass (g)	δm (g)	Matl	Mass (g)	Ignition (yes/no)
186	4080AV	BKN	.6	.1	NACO	40	No
187	4080AV	BKN	.7	.1	NACO	40	Yes
188	4080AV	BKN	.6	.1	NACO	40	No
189	4080AV	BKN	.7	.1	NACO	40	Yes
190	4080AV	BKN	.6	.1	NACO	40	No
191	4080AV	BKN	.7	.1	NACO	40	Yes
192	4080AV	BKN	.6	.1	NACO	40	No
193	4080AV	BKN	.7	.1	NACO	40	No
194	4080AV	BKN	.8	.1	NACO	40	Yes
195	4080AV	BKN	.7	.1	NACO	40	Yes
196	4080AV	BKN	.6	.1	NACO	40	No

IECD IGNITION EFFECTIVENESS TEST DATA

(Inert Simulant Zone 1 Thickness 1.00 in)

	Igniter				Propellant		
Test Number	Configuration	Matl	Mass (g)	δm (g)	Matl	Mass (g)	Ignition (yes/no)
1001	4080AV	NC	2.0	.5	NACO	40	Yes
1002	4080AV	NC	1.5	.5	NACO	40	No
1003	4080AV	NC	2.0	.2	NACO	40	Yes
1004	4080AV	NC	1.8	.2	NACO	40	Yes
1005	4080AV	NC	1.6	.2	NACO	40	Yes
1006	4080AV	NC	1.4	.2	NACO	40	Yes
1007	4080AV	NC	1.2	.2	NACO	40	Yes
1008	4080AV	NC	1.0	.2	NACO	40	No
1009	4080AV	NC	1.2	.2	NACO	40	No
1010	4080AV	NC	1.2	.2	NACO	40	Yes
1011	4080AV	NC	1.0	.2	NACO	40	No
1012	4080AV	NC	1.2	.2	NACO	40	Yes
1013	4080AV	NC	1.0	.2	NACO	40	No
1014	4080AV	NC	1.2	.2	NACO	40	No
1015	4080AV	NC	1.2	.2	NACO	40	No
1016	4080AV	NC	1.2	.2	NACO	40	Yes
1017	4080AV	NC	1.0	.2	NACO	40	No
1018	4080AV	NC	1.2	.2	NACO	40	Yes
1019	4080AV	NC	1.0	.2	NACO	40	No
1020	4080AV	NC	1.2	.2	NACO	40	No
1021	4080AV	NC	1.2	.2	NACO	40	Yes

IECD IGNITION EFFECTIVENESS TEST DATA

(Inert Simulant Zone 1 Thickness 1.00 in)

	Igniter				Propellant		
Test Number	Configuration	Matl	Mass (g)	δm (g)	Matl	Mass (g)	Ignition (yes/no)
1095	4080AV	BMO	4.0	.5	NACO	40	No
1096	4080AV	BMO	4.5	.5	NACO	40	Yes
1097	4080AV	BMO	4.0	.5	NACO	40	Yes
1098	4080AV	BMO	3.5	.5	NACO	40	No
1099	4080AV	BMO	4.0	.5	NACO	40	Yes
1100	4080AV	BMO	3.5	.5	NACO	40	Yes
1101	4080AV	BMO	3.0	.5	NACO	40	No
1102	4080AV	BMO	3.5	.5	NACO	40	No
1103	4080AV	BMO	4.0	.5	NACO	40	Yes
1104	4080AV	BMO	3.5	.5	NACO	40	Yes
1105	4080AV	BMO	3.0	.5	NACO	40	No

IECD IGNITION EFFECTIVENESS TEST DATA

(Inert Simulant Zone 1 Thickness 1.00 in)

	Igniter				Propellant		
Test Number	Configuration	Matl	Mass (g)	δm (g)	Matl	Mass (g)	Ignition (yes/no)
2001	4080AV	BKN	1.4	.2	N318	40	Yes
2002	4080AV	BKN	1.2	.2	N318	40	No
2003	4080AV	BKN	1.4	.2	N318	40	No
2004	4080AV	BKN	1.6	.2	N318	40	No
2005	4080AV	BKN	1.8	.2	N318	40	No
2006	4080AV	BKN	2.0	.2	N318	40	No
2007	4080AV	BKN	2.2	.2	N318	40	Yes
2008	4080AV	BKN	2.0	.2	N318	40	Yes
2009	4080AV	BKN	1.8	.2	N318	40	Yes
2010	4080AV	BKN	1.6	.2	N318	40	No
2011	4080AV	BKN	1.8	.2	N318	40	No
2012	4080AV	BKN	2.0	.2	N318	40	Yes
2013	4080AV	BKN	1.8	.2	N318	40	No
2014	4080AV	BKN	2.0	.2	N318	40	Yes

IECD IGNITION EFFECTIVENESS TEST DATA

(Inert Simulant Zone 1 Thickness 1.00 in)

	Igniter				Propellant		
Test Number	Configuration	Matl	Mass (g)	δm (g)	Matl	Mass (g)	Ignition (yes/no)
2015	4080AV	NC	2.3	.3	N318	40	Yes
2016	4080AV	NC	2.0	.3	N318	40	Yes
2017	4080AV	NC	1.7	.3	N318	40	Yes
2018	4080AV	NC	1.4	.3	N318	40	No
2019	4080AV	NC	1.7	.3	N318	40	Yes
2020	4080AV	NC	1.4	.3	N318	40	No
2021	4080AV	NC	1.7	.3	N318	40	Yes
2022	4080AV	NC	1.4	.3	N318	40	Yes
2023	4080AV	NC	1.1	.3	N318	40	Yes
2024	4080AV	NC	.8	.3	N318	40	No
2025	4080AV	NC	1.1	.3	N318	40	No
2026	4080AV	NC	1.4	.3	N318	40	Yes
2027	4080AV	NC	1.1	.3	N318	40	No

IECD IGNITION EFFECTIVENESS TEST DATA

(Inert Simulant Zone 1 Thickness 1.00 in)

	Igniter			Propellant		
Configuration	Matl	Mass (g)	δm (g)	Matl	Mass (g)	Ignition (yes/no)
5113	BP	3.5	.5	LOVA	40	No
5113	BP	4.0	.5	LOVA	40	Yes
5113	BP	3.5	.5	LOVA	40	No
5113	BP	4.0	.5	LOVA	40	Yes
5113	BP	3.5	.3	LOVA	40	No
5113	BP	3.8	.3	LOVA	40	No
5113	BP	4.1	.3	LOVA	40	Yes
5113	BP	3.8	.3	LOVA	40	No
5113	BP	4.1	.3	LOVA	40	No
5113	BP	4.4	.3	LOVA	40	Yes
5113	BP	4.1	.3	LOVA	40	Yes
5113	BP	3.8	.3	LOVA	40	No
5113	BP	4.1	.3	LOVA	40	Yes
5113	BP	3.8	.3	LOVA	40	No
5113	BP	4.1	.3	LOVA	40	No

IECD IGNITION EFFECTIVENESS TEST DATA

(Inert Simulant Zone 1 Thickness 1.00 in)

	Igniter				Propellant		
Test Number	Configuration	Matl	Mass (g)	δm (g)	Matl	Mass (g)	Ignition (yes/no)
4100	5113	BKN	2.4	.3	LOVA	40	Yes
4101	5113	BKN	2.1	.3	LOVA	40	No
4102	5113	BKN	2.4	.3	LOVA	40	Yes
4103	5113	BKN	2.1	.3	LOVA	40	Yes
4104	5113	BKN	1.8	.3	LOVA	40	No
4105	5113	BKN	2.1	.3	LOVA	40	No
4106	5113	BKN	2.4	.3	LOVA	40	Yes
4107	5113	BKN	2.1	.3	LOVA	40	Yes
4108	5113	BKN	1.8	.3	LOVA	40	No
4109	5113	BKN	2.1	.3	LOVA	40	Yes
4110	5113	BKN	1.8	.3	LOVA	40	No

IECD IGNITION EFFECTIVENESS TEST DATA

(Inert Simulant Zone 1 Thickness 0.00 in)

	Igniter				Propellant		
Test Number	Configuration	Matl	Mass (g)	δm (g)	Matl	Mass (g)	Ignition (yes/no)
4111	5113	BMO	5.0	1.0	LOVA	40	No
4112	5113	BMO	6.0	2.0	LOVA	40	No
4113	5113	BMO	8.0	2.0	LOVA	40	No
4114	5113	BMO	10.0	5.0	LOVA	40	No
4115	5113	BMO	15.0	-	LOVA	40	No
4116	5113	BMO/NC	6.0	1.0	LOVA	40	No
4117	5113	BMO/NC	6.0	2.0	LOVA	40	No

IECD IGNITION EFFECTIVENESS TEST DATA

(Inert Simulant Zone 1 Thickness 1.00 in)

	Igniter				Propellant		
Test Number	Configuration	Matl	Mass (g)	δm (g)	Matl	Mass (g)	Ignition (yes/no)
4118	5113	MTV	2.0	.3	LOVA	40	No
4119	5113	MTV	2.3	.3	LOVA	40	Yes
4120	5113	MTV	2.0	.3	LOVA	40	No
4121	5113	MTV	2.3	.3	LOVA	40	Yes
4122	5113	MTV	2.0	.2	LOVA	40	Yes
4123	5113	MTV	1.8	.2	LOVA	40	No
4124	5113	MTV	2.0	.2	LOVA	40	Yes
4125	5113	MTV	1.8	.2	LOVA	40	No
4126	5113	MTV	2.0	.2	LOVA	40	Yes
4127	5113	MTV	1.8	.2	LOVA	40	No
4128	5113	MTV	2.0	.2	LOVA	40	Yes
4129	5113	MTV	1.8	.2	LOVA	40	No
4130	5113	MTV	2.0	.2	LOVA	40	No
4131	5113	MTV	2.2	.2	LOVA	40	Yes
4132	5113	MTV	2.0	.2	LOVA	40	No

IECD IGNITION EFFECTIVENESS TEST DATA

(Inert Simulant Zone 1 Thickness 1.50 in)

	Igniter				Propellant		
Test Number	Configuration	Matl	Mass (g)	δm (g)	Matl	Mass (g)	Ignition (yes/no)
101E	4080AV-R	BP	.6	.1	NACO	40	No
102E	4080AV-R	BP	.7	.1	NACO	40	No
103E	4080AV-R	BP	.8	.1	NACO	40	No
104E	4080AV-R	BP	.9	.1	NACO	40	No
105E	4080AV-R	BP	1.0	.1	NACO	40	No
106E	4080AV-R	BP	1.31	.1	NACO	40	No
107E	4080AV	BP	1.31	.1	NACO	40	Yes
108E	4080AV	BP	1.0	.1	NACO	40	Yes
101	4080AV	BP	.7	.1	NACO	40	No
102	4080AV	BP	.8	.1	NACO	40	No
103	4080AV	BP	.9	.1	NACO	40	Yes
104	4080AV	BP	.8	.1	NACO	40	No
105	4080AV	BP	.9	.1	NACO	40	No
106	4080AV	BP	1.0	.1	NACO	40	No
107	4080AV	BP	1.1	.1	NACO	40	Yes
108	4080AV	BP	1.0	.1	NACO	40	No
109	4080AV	BP	1.1	.1	NACO	40	No
110	4080AV	BP	1.2	.1	NACO	40	No
111	4080AV	BP	1.3	.1	NACO	40	No
112	4080AV	BP	1.4	.1	NACO	40	No
113	4080AV	BP	1.5	.1	NACO	40	No
114	4080AV	BP	1.6	.1	NACO	40	No
115	4080AV	BP	1.2	.3	NACO	40	No
116	4080AV	BP	1.5	.3	NACO	40	No
117	4080AV	BP	1.8	.3	NACO	40	No
118	4080AV	BP	2.1	.3	NACO	40	Yes
119	4080AV	BP	1.8	.3	NACO	40	Yes
120	4080AV	BP	1.5	.3	NACO	40	No
121	4080AV	BP	1.8	.3	NACO	40	Yes
122	4080AV	BP	1.5	.3	NACO	40	Yes
123	4080AV	BP	1.2	.3	NACO	40	No

IECD IGNITION EFFECTIVENESS TEST DATA

(Inert Simulant Zone 1 Thickness 1.50 in)

	Igniter				Propellant		
Test Number	Configuration	Matl	Mass (g)	δm (g)	Matl	Mass (g)	Ignition (yes/no)
124	4080AV	BKN	.8	.2	NACO	40	Yes
125	4080AV	BKN	.6	.2	NACO	40	No
126	4080AV	BKN	.8	.2	NACO	40	No
127	4080AV	BKN	1.0	.2	NACO	40	No
128	4080AV	BKN	1.2	.2	NACO	40	Yes
129	4080AV	BKN	1.0	.2	NACO	40	Yes
130	4080AV	BKN	.8	.2	NACO	40	No
131	4080AV	BKN	1.0	.2	NACO	40	Yes
132	4080AV	BKN	.8	.2	NACO	40	Yes

IECD IGNITION EFFECTIVENESS TEST DATA

(Inert Simulant Zone 1 Thickness 1.50 in)

	Igniter				Propellant		
Test Number	Configuration	Matl	Mass (g)	δm (g)	Matl	Mass (g)	Ignition (yes/no)
133	4080AV	NC	1.4	.3	NACO	40	No
134	4080AV	NC	1.7	.3	NACO	40	No
135	4080AV	NC	2.0	.3	NACO	40	No
136	4080AV	NC	2.3	.3	NACO	40	No
137	4080AV	NC	2.6	.3	NACO	40	Yes
138	4080AV	NC	2.3	.3	NACO	40	Yes
139	4080AV	NC	2.0	.3	NACO	40	No
140	4080AV	NC	2.3	.3	NACO	40	Yes
141	4080AV	NC	2.0	.3	NACO	40	No
142	4080AV	NC	2.3	.3	NACO	40	No
143	4080AV	NC	2.6	.3	NACO	40	No
144	4080AV	NC	2.9	.3	NACO	40	Yes

IECD IGNITION EFFECTIVENESS TEST DATA

(Inert Simulant Zone 1 Thickness 1.50 in)

	Igniter				Propellant		
Test Number	Configuration	Matl	Mass (g)	δm (g)	Matl	Mass (g)	Ignition (yes/no)
145	4080AV	MTV	1.2	.8	NACO	40	No
146	4080AV	MTV	2.0	.3	NACO	40	Yes
147	4080AV	MTV	1.7	.3	NACO	40	Yes
148	4080AV	MTV	1.4	.3	NACO	40	Yes
149	4080AV	MTV	1.1	.3	NACO	40	No
150	4080AV	MTV	1.4	.3	NACO	40	Yes
151	4080AV	MTV	1.1	.3	NACO	40	No
152	4080AV	MTV	1.4	.3	NACO	40	Yes
153	4080AV	MTV	1.1	.3	NACO	40	Yes
154	4080AV	MTV	.8	.3	NACO	40	No
155	4080AV	MTV	1.1	.3	NACO	40	Yes
156	4080AV	MTV	.8	.3	NACO	40	No

IECD IGNITION EFFECTIVENESS TEST DATA

(Inert Simulant Zone 1 Thickness 1.50 in)

	Igniter				Propellant		
Test Number	Configuration	Matl	Mass (g)	δm (g)	Matl	Mass (g)	Ignition (yes/no)
157	4080AV	BMO	3.0	.5	NACO	40	No
158	4080AV	BMO	5.0	.5	NACO	40	Yes
159	4080AV	BMO	4.0	.5	NACO	40	No
160	4080AV	BMO	4.5	.5	NACO	40	No
161	4080AV	BMO	5.0	.5	NACO	40	No
162	4080AV	BMO	5.5	.5	NACO	40	No
163	4080AV	BMO	6.0	.5	NACO	40	Yes
164	4080AV	BMO	5.5	.5	NACO	40	Yes
165	4080AV	BMO	5.0	.5	NACO	40	No
166	4080AV	BMO	5.5	.5	NACO	40	Yes
167	4080AV	BMO	5.0	.5	NACO	40	No
168	4080AV	BMO	5.5	.5	NACO	40	No
169	4080AV	BMO	6.0	.5	NACO	40	No
170	4080AV	BMO	6.5	.5	NACO	40	Yes
171	4080AV	BMO	6.0	.5	NACO	40	No
172	4080AV	BMO	6.5	.5	NACO	40	No

IECD IGNITION EFFECTIVENESS TEST DATA

(Inert Simulant Zone 1 Thickness 1.50 in)

	Igniter				Propellant			
Test Number	Configuration	Matl	Mass (g)	δm (g)	Matl	Mass (g)	Ignition (yes/no)	
201	4080AV	BP	1.65	.6	N318	40	No	
202	4080AV	BP	2.25	.6	N318	40	Yes	
203	4080AV	BP	1.65	.6	N318	40	No	
204	4080AV	BP	2.25	.6	N318	40	No	
205	4080AV	BP	2.85	.6	N318	40	No	
206	4080AV	BP	3.45	.6	N318	40	No	
207	4080AV	BP	4.05	.6	N318	40	No	
208	4080AV	BP	3.45	-	NACO	40	Yes	Zone 1
209	4080AV	BP	2.00	-	N318	40	No	Thickness
210	4080AV	BP	3.00	-	N318	40	Yes	0.0 in
211	4080AV	BP	4.65	.6	N318	40	No	
212	4080AV	BP	5.25	.6	N318	40	Yes	
213	4080AV	BP	4.65	.6	N318	40	No	
214	4080AV	BP	5.25	.6	N318	40	Yes	
215	4080AV	BP	4.65	.6	N318	40	Yes	
216	4080AV	BP	4.05	.6	N318	40	No	
217			No Test Conducted					
218	4080AV	BP	4.70	.3	N318	40	No	
219	4080AV	BP	5.00	.3	N318	40	Yes	
220	4080AV	BP	4.70	.3	N318	40	Yes	
221	4080AV	BP	4.40	.3	N318	40	No	
222	4080AV	BP	4.70	.3	N318	40	Yes	
223	4080AV	BP	4.40	.3	N318	40	No	
224	4080AV	BP	4.70	.3	N318	40	Yes	
225	4080AV	BP	4.40	.3	N318	40	Yes	
226	4080AV	BP	4.10	.3	N318	40	Yes	
227	4080AV	BP	3.80	.3	N318	40	Yes	
228	4080AV	BP	3.50	.3	N318	40	No	
229	4080AV	BP	3.80	.3	N318	40	Yes	

IECD IGNITION EFFECTIVENESS TEST DATA

(Inert Simulant Zone 1 Thickness 1.50 in)

	Igniter				Propellant		
Test Number	Configuration	Matl	Mass (g)	δm (g)	Matl	Mass (g)	Ignition (yes/no)
230	4080AV	BKN	2.0	.5	N318	40	No
231	4080AV	BKN	2.5	.5	N318	40	Yes
232	4080AV	BKN	2.0	.5	N318	40	No
233	4080AV	BKN	2.5	.2	N318	40	Yes
234	4080AV	BKN	2.3	.2	N318	40	Yes
235	4080AV	BKN	2.1	.2	N318	40	Yes
236	4080AV	BKN	1.9	.2	N318	40	No
237	4080AV	BKN	2.1	.2	N318	40	Yes
238	4080AV	BKN	1.9	.2	N318	40	Yes
239	4080AV	BKN	1.7	.2	N318	40	No
240	4080AV	BKN	1.9	.2	N318	40	Yes
241	4080AV	BKN	1.7	.2	N318	40	No
242	4080AV	BKN	1.9	.2	N318	40	Yes
243	4080AV	BKN	1.7	.2	N318	40	Yes
244	4080AV	BKN	1.5	.2	N318	40	No
245	4080AV	BKN	1.7	.2	N318	40	Yes

IECD IGNITION EFFECTIVENESS TEST DATA

(Inert Simulant Zone 1 Thickness 1.50 in)

	Igniter				Propellant		
Test Number	Configuration	Matl	Mass (g)	δm (g)	Matl	Mass (g)	Ignition (yes/no)
246	4080AV	NC	5.0	1.0	N318	40	Yes
247	4080AV	NC	4.0	1.0	N318	40	Yes
248	4080AV	NC	3.0	1.0	N318	40	Yes
249	4080AV	NC	2.0	1.0	N318	40	No
250	4080AV	NC	2.3	.3	N318	40	No
251	4080AV	NC	2.6	.3	N318	40	No
252	4080AV	NC	2.9	.3	N318	40	No
253	4080AV	NC	3.2	.3	N318	40	Yes
254	4080AV	NC	2.9	.3	N318	40	No
255	4080AV	NC	3.2	.3	N318	40	Yes
256	4080AV	NC	2.9	.3	N318	40	No
257	4080AV	NC	3.2	.3	N318	40	No
258	4080AV	NC	3.5	.3	N318	40	Yes
259	4080AV	NC	3.2	.3	N318	40	Yes
260	4080AV	NC	2.9	.3	N318	40	Yes
261	4080AV	NC	2.6	.3	N318	40	No

IECD IGNITION EFFECTIVENESS TEST DATA

(Inert Simulant Zone 1 Thickness 1.50 in)

	Igniter				Propellant		
Test Number	Configuration	Matl	Mass (g)	δm (g)	Matl	Mass (g)	Ignition (yes/no)
262	4080AV	MTV	2.0	.3	N318	40	Yes
263	4080AV	MTV	1.7	.3	N318	40	Yes
264	4080AV	MTV	1.4	.3	N318	40	No
265	4080AV	MTV	1.7	.3	N318	40	Yes
266	4080AV	MTV	1.4	.3	N318	40	No
267	4080AV	MTV	1.7	.3	N318	40	No
268	4080AV	MTV	2.0	.3	N318	40	Yes
269	4080AV	MTV	1.7	.3	N318	40	Yes
270	4080AV	MTV	1.4	.3	N318	40	No
271	4080AV	MTV	1.7	.3	N318	40	Yes

IECD IGNITION EFFECTIVENESS TEST DATA

(Inert Simulant Zone 1 Thickness 1.50 in)

	Igniter				Propellant		
Test Number	Configuration	Matl	Mass (g)	δm (g)	Matl	Mass (g)	Ignition (yes/no)
301	4080AV	BP	1.8	.5	N363	39.2	No
302	4080AV	BP	2.3	.5	N363	39.2	No
303	4080AV	BP	2.8	.5	N363	39.2	No
304	4080AV	BP	3.3	.5	N363	39.2	No
305	4080AV	BP	3.8	.5	N363	39.2	No
306	4080AV	BP	4.3	.5	N363	39.2	NO
307	4080AV	BP	4.8	.5	N363	39.2	Yes
308	4080AV	BP	4.3	.5	N363	39.2	No
309	4080AV	BP	4.8	.5	N363	39.2	Yes
310	4080AV	BP	4.6	.3	N363	39.2	No
311	4080AV	BP	4.9	.3	N363	39.2	Yes
312	4080AV	BP	4.6	.3	N363	39.2	No
313	4080AV	BP	4.9	.3	N363	39.2	No
314	4080AV	BP	5.2	.3	N363	39.2	Yes
315	4080AV	BP	4.9	.3	N363	39.2	Yes
316	4080AV	BP	4.6	.3	N363	39.2	Yes
317	4080AV	BP	4.3	.3	N363	39.2	No
318	4080AV	BP	4.6	.3	N363	39.2	No
319	4080AV	BP	4.9	.3	N363	39.2	Yes
320	4080AV	BP	4.6	.3	N363	39.2	No
321	4080AV	BP	4.9	.3	N363	39.2	Yes

IBCD IGNITION EFFECTIVENESS TEST DATA

(Inert Simulant Zone 1 Thickness 1.50 in)

	Igniter				Propellant		
Test Number	Configuration	Matl	Mass (g)	δm (g)	Matl	Mass (g)	Ignition (yes/no)
322	4080AV	BKN	2.5	.5	N363	39.2	Yes
323	4080AV	BKN	2.0	.5	N363	39.2	No
324	4080AV	BKN	2.5	.5	N363	39.2	No
325	4080AV	BKN	3.0	.5	N363	39.2	No
326	4080AV	BKN	3.5	.5	N363	39.2	No
327	4080AV	BKN	4.0	.5	N363	39.2	Yes
328	4080AV	BKN	3.5	.5	N363	39.2	Yes
329	4080AV	BKN	3.0	.3	N363	39.2	Yes
330	4080AV	BKN	2.7	.3	N363	39.2	Yes
331	4080AV	BKN	2.4	.3	N363	39.2	No
332	4080AV	BKN	2.7	.3	N363	39.2	Yes
333	4080AV	BKN	3.4	.3	N363	39.2	Yes
334	4080AV	BKN	2.4	.3	N363	39.2	No
335	4080AV	BKN	2.7	.3	N363	39.2	No
336	4080AV	BKN	3.0	.3	N363	39.2	No
337	4080AV	BKN	3.3	.3	N363	39.2	Yes
338	4080AV	BKN	3.0	.3	N363	39.2	No
339	4080AV	BKN	3.3	.3	N363	39.2	Yes
340	4080AV	BKN	3.0	.3	N363	39.2	Yes

IECD IGNITION EFFECTIVENESS TEST DATA

(Inert Simulant Zone 1 Thickness 1.50 in)

	Igniter				Propellant		
Test Number	Configuration	Matl	Mass (g)	δm (g)	Matl	Mass (g)	Ignition (yes/no)
341	4080AV	NC	3.5	.5	N363	39.2	No
342	4080AV	NC	4.0	.5	N363	39.2	Yes
343	4080AV	NC	3.5	.5	N363	39.2	No
344	4080AV	NC	4.0	.5	N363	39.2	Yes
345	4080AV	NC	3.5	.5	N363	39.2	Yes
346	4080AV	NC	3.0	.5	N363	39.2	No
347	4080AV	NC	3.3	.3	N363	39.2	No
348	4080AV	NC	3.6	.3	N363	39.2	No
349	4080AV	NC	3.9	.3	N363	39.2	Yes
350	4080AV	NC	3.6	.3	N363	39.2	Yes
351	4080AV	NC	3.3	.3	N363	39.2	No
352	4080AV	NC	3.6	.3	N363	39.2	Yes
353	4080AV	NC	3.3	.3	N363	39.2	No
354	4080AV	NC	3.6	.3	N363	39.2	Yes
355	4080AV	NC	3.3	.3	N363	39.2	No
356	4080AV	NC	3.6	.3	N363	39.2	No
357	4080AV	NC	3.9	.3	N363	39.2	Yes

IECD IGNITION EFFECTIVENESS TEST DATA

(Inert Simulant Zone 1 Thickness 1.50 in)

	Igniter				Propellant		
Test Number	Configuration	Matl	Mass (g)	δm (g)	Matl	Mass (g)	Ignition (yes/no)
358	4080AV	MTV	3.0	.3	N363	39.2	Yes
359	4080AV	MTV	2.7	.3	N363	39.2	Yes
360	4080AV	MTV	2.4	.3	N363	39.2	No
361	4080AV	MTV	2.7	.3	N363	39.2	No
362	4080AV	MTV	3.0	.3	N363	39.2	Yes
363	4080AV	MTV	2.7	.3	N363	39.2	Yes
364	4080AV	MTV	2.4	.3	N363	39.2	No
365	4080AV	MTV	2.7	.3	N363	39.2	No
366	4080AV	MTV	3.0	.3	N363	39.2	Yes
367	4080AV	MTV	2.7	.3	N363	39.2	Yes

IECD IGNITION EFFECTIVENESS TEST DATA

(LOVA EXPLORATORY)

(Inert Simulant Zone 1 Thickness 1.50 in)

	Igniter				Propellant		
Test Number	Configuration	Matl	Mass (g)	δm (g)	Matl	Mass (g)	Ignition (yes/no)
401	4080AV	BP	4.5	.5	LOVA	40	No
402	4080AV	BP	5.0	.5	LOVA	40	No
403	4080AV	BP	5.5	.5	LOVA	40	No
404	4080AV	BP	6.0	.5	LOVA	40	No
405	4080AV	BP	7.0	1.0	LOVA	40	No
406	4080AV	BKN	3.0	1.0	LOVA	40	No
407	4080AV	BKN	4.0	1.0	LOVA	40	No
408	4080AV	BKN	5.0	1.0	LOVA	40	No
409	4080AV	NC	5.0	1.0	LOVA	40	No
410	4080AV	BKN	5.0	0	LOVA	40	No
411	5113	BKN	5.0	2.0	LOVA	40	Yes
412	5113	BKN	3.0	1.0	LOVA	40	No
413	5113	BKN	4.0	1.0	LOVA	40	No
414	4113-205	BKN	4.0	1.0	LOVA	40	No
415	4113-205	BKN	5.0	1.0	LOVA	40	No
416	5113	BKN	5.0	1.0	LOVA	40	No
417	5113	BKN	6.0	1.0	LOVA	40	Yes
418	5113	BKN	5.0	1.0	LOVA	40	Yes
419	5113	BKN	4.0	1.0	LOVA	40	Yes
420	5113	BKN	2.0	1.0	LOVA	40	No
421	5113	BKN	3.0	1.0	LOVA	40	Yes
422	5113	BKN	4.0	1.0	LOVA	40	Yes
423	5113	BKN	3.0	1.0	LOVA	40	Yes
424	5113	BKN	2.5	.5	LOVA	40	Yes
425	5113	BKN	2.5	.5	LOVA	40	Yes
426	5113	BKN	3.0	1.0	LOVA	40	Yes
427	5113	BKN	4.0	1.0	LOVA	40	Yes
428	5113	BKN	2.5	.5	LOVA	40	Yes
429	5113	BKN	3.0	.5	LOVA	40	Yes

IECD IGNITION EFFECTIVENESS TEST DATA

(LOVA EXPLORATORY)

(Inert Simulant Zone 1 Thickness 1.50 in)

	Igniter				Propellant		
Test Number	Configuration	Matl	Mass (g)	δm (g)	Matl	Mass (g)	Ignition (yes/no)
430	5113	BKN	2.5	.5	LOVA	40	No
431	5113	BKN	3.0	.5	LOVA	40	Yes
432	5113	BKN	2.5	.5	LOVA	40	Yes
433	5113	BKN	2.0	.5	LOVA	40	No
434	5113	BKN	2.5	.5	LOVA	40	No
435	5113	BKN	3.0	.5	LOVA	40	Yes
436	5113	BKN	2.5	.5	LOVA	40	Yes
437	5113	BKN	2.0	.5	LOVA	40	No
438	5113	BKN	2.5	.5	LOVA	40	No
439	5113	BKN	3.0	.5	LOVA	40	Yes

IECD IGNITION EFFECTIVENESS TEST DATA

(Inert Simulant Zone 1 Thickness 1.50 in)

	Igniter				Propellant		
Test Number	Configuration	Matl	Mass (g)	δm (g)	Matl	Mass (g)	Ignition (yes/no)
440	5113	BP	6.0	1	LOVA	40	No
441	5113	BP	7.0	1	LOVA	40	Yes
442	5113	BP	6.0	1	LOVA	40	Yes
443	5113	BP	5.0	1	LOVA	40	Yes
444	5113	BP	4.0	1	LOVA	40	No
445	5113	BP	5.0	1	LOVA	40	No
446	5113	BP	6.0	1	LOVA	40	No
447	5113	BP	7.0	1	LOVA	40	Yes
448	5113	BP	6.0	1	LOVA	40	Yes
449	5113	BP	5.0	1	LOVA	40	Yes

IECD IGNITION EFFECTIVENESS TEST DATA

(Inert Simulant Zone 1 Thickness 1.50 in)

	Igniter				Propellant		
Test Number	Configuration	Matl	Mass (g)	δm (g)	Matl	Mass (g)	Ignition (yes/no)
450	5113	MTV	3.0	.5	LOVA	40	No
451	5113	MTV	3.5	.5	LOVA	40	Yes
452	5113	MTV	3.0	.5	LOVA	40	Yes
453	5113	MTV	2.5	.5	LOVA	40	No
454	5113	MTV	3.0	.5	LOVA	40	Yes
455	5113	MTV	2.5	.5	LOVA	40	No
456	5113	MTV	3.0	.5	LOVA	40	No
457	5113	MTV	3.5	.5	LOVA	40	Yes
458	5113	MTV	3.0	.5	LOVA	40	Yes
459	5113	MTV	2.5	.5	LOVA	40	No

IECD IGNITION EFFECTIVENESS TEST DATA

(Inert Simulant Zone 1 Thickness 1.50 in)

	Igniter				Propellant		
Test Number	Configuration	Matl	Mass (g)	δm (g)	Matl	Mass (g)	Ignition (yes/no)
460	5113	NC	4.0	1	LOVA	40	No
461	5113	NC	5.0	1	LOVA	40	Yes
462	5113	NC	4.0	1	LOVA	40	Yes
463	5113	NC	3.0	1	LOVA	40	No
464	5113	NC	4.0	1	LOVA	40	No
465	5113	NC	5.0	1	LOVA	40	Yes
466	5113	NC	4.0	1	LOVA	40	No
467	5113	NC	5.0	1	LOVA	40	Yes
468	5113	NC	4.0	1	LOVA	40	No
469	5113	NC	5.0	1	LOVA	40	Yes

IECD IGNITION EFFECTIVENESS TEST DATA

(Inert Simulant Zone 1 Thickness 1.50 in)

	Igniter				Propellant		
Test Number	Configuration	Matl	Mass (g)	δm (g)	Matl	Mass (g)	Ignition (yes/no)
4070	4080	NC	3.0	.5	PYRO	40	No
4071	4080	NC	3.5	.5	PYRO	40	No
4072	4080	NC	4.0	.5	PYRO	40	Yes
4073	4080	NC	3.5	.5	PYRO	40	No
4074	4080	NC	4.0	.4	PYRO	40	Yes
4075	4080	NC	3.6	.4	PYRO	40	Yes
4076	4080	NC	3.2	.4	PYRO	40	Yes
4077	4080	NC	2.8	.4	PYRO	40	No
4078	4080	NC	3.2	.4	PYRO	40	Yes
4079	4080	NC	2.8	.4	PYRO	40	No
4080	4080	NC	3.2	.4	PYRO	40	Yes
4081	4080	NC	2.8	.4	PYRO	40	No
4082	4080	NC	3.2	.4	PYRO	40	Yes
4083	4080	NC	2.8	.4	PYRO	40	No
4084	4080	NC	3.2	.4	PYRO	40	No

IECD IGNITION EFFECTIVENESS TEST DATA

(Inert Simulant Zone 1 Thickness 1.50 in)

	Igniter				Propellant		
Test Number	Configuration	Matl	Mass (g)	δm (g)	Matl	Mass (g)	Ignition (yes/no)
4147	5113	AP	2.5	.3	LOVA	40	No
4148	5113	AP	2.8	.3	LOVA	40	No
4149	5113	AP	3.1	.3	LOVA	40	Yes
4150	5113	AP	2.8	.3	LOVA	40	Yes
4151	5113	AP	2.5	.3	LOVA	40	No
4152	5113	AP	2.8	.3	LOVA	40	Yes
4153	5113	AP	2.5	.3	LOVA	40	Yes
4154	5113	AP	2.2	.3	LOVA	40	No
4155	5113	AP	2.5	.3	LOVA	40	Yes
4156	5113	AP	2.2	.3	LOVA	40	No
4157	5113	AP	2.5	.3	LOVA	40	Yes
4158	5113	AP	2.2	.3	LOVA	40	Yes

IECD IGNITION EFFECTIVENESS TEST DATA

(Inert Simulant Zone 1 Thickness 2.00 in)

	Igniter				Propellant		
Test Number	Configuration	Matl	Mass (g)	δm (g)	Matl	Mass (g)	Ignition (yes/no)
1022	4080AV	BP	2.2	.4	NACO	40	No
1023	4080AV	BP	2.6	.4	NACO	40	No
1024	4080AV	BP	3.0	.4	NACO	40	No
1025	4080AV	BP	3.4	.4	NACO	40	Yes
1026	4080AV	BP	3.0	.4	NACO	40	Yes
1027	4080AV	BP	2.6	.4	NACO	40	No
1028	4080AV	BP	3.0	.2	NACO	40	Yes
1029	4080AV	BP	2.8	.2	NACO	40	Yes
1030	4080AV	BP	2.6	.2	NACO	40	Yes
1031	4080AV	BP	2.4	.2	NACO	40	No
1032	4080AV	BP	2.6	.2	NACO	40	No
1033	4080AV	BP	2.8	.2	NACO	40	No
1034	4080AV	BP	3.0	.2	NACO	40	Yes
1035	4080AV	BP	2.8	.2	NACO	40	No
1036	4080AV	BP	3.0	.2	NACO	40	Yes
1037	4080AV	BP	2.8	.2	NACO	40	No
1038	4080AV	BP	3.0	.2	NACO	40	No

IECD IGNITION EFFECTIVENESS TEST DATA

(Inert Simulant Zone 1 Thickness 2.00 in)

	Igniter				Propellant		
Test Number	Configuration	Matl	Mass (g)	δm (g)	Matl	Mass (g)	Ignition (yes/no)
1039	4080AV	BKN	1.2	.2	NACO	40	Yes
1040	4080AV	BKN	1.0	.2	NACO	40	No
1041	4080AV	BKN	1.2	.1	NACO	40	Yes
1042	4080AV	BKN	1.1	.1	NACO	40	No
1043	4080AV	BKN	1.2	.1	NACO	40	Yes
1044	4080AV	BKN	1.1	.1	NACO	40	No
1045	4080AV	BKN	1.2	.1	NACO	40	Yes
1046	4080AV	BKN	1.1	.1	NACO	40	Yes
1047	4080AV	BKN	1.0	.1	NACO	40	Yes
1048	4080AV	BKN	.9	.1	NACO	40	No
1049	4080AV	BKN	1.0	.1	NACO	40	No
1050	4080AV	BKN	1.1	.1	NACO	40	Yes
1051	4080AV	BKN	1.0	.1	NACO	40	Yes

IECD IGNITION EFFECTIVENESS TEST DATA

(Inert Simulant Zone 1 Thickness 2.00 in)

	Igniter				Propellant		
Test Number	Configuration	Matl	Mass (g)	δm (g)	Matl	Mass (g)	Ignition (yes/no)
1052	4080AV	NC	2.0	.5	NACO	40	No
1053	4080AV	NC	2.5	.5	NACO	40	No
1054	4080AV	NC	3.0	.5	NACO	40	No
1055	4080AV	NC	3.5	.5	NACO	40	Yes
1056	4080AV	NC	3.0	.5	NACO	40	Yes
1057	4080AV	NC	2.5	.5	NACO	40	Yes
1058	4080AV	NC	2.0	.5	NACO	40	No
1059	4080AV	NC	2.5	.5	NACO	40	No
1060	4080AV	NC	3.0	.5	NACO	40	Yes
1061	4080AV	NC	2.5	.5	NACO	40	No
1062	4080AV	NC	3.0	.5	NACO	40	No
1063	4080AV	NC	3.5	.5	NACO	40	Yes

IECD IGNITION EFFECTIVENESS TEST DATA

(Inert Simulant Zone 1 Thickness 2.00 in)

Test Number	Igniter Configuration	Igniter Matl	Igniter Mass (g)	δm (g)	Propellant Matl	Propellant Mass (g)	Ignition (yes/no)
1064	4080AV	MTV	1.2	.2	NACO	40	No
1065	4080AV	MTV	1.4	.2	NACO	40	Yes
1066	4080AV	MTV	1.2	.2	NACO	40	Yes
1067	4080AV	MTV	1.0	.1	NACO	40	Yes
1068	4080AV	MTV	.9	.1	NACO	40	No
1069	4080AV	MTV	1.0	.1	NACO	40	No
1070	4080AV	MTV	1.1	.1	NACO	40	Yes
1071	4080AV	MTV	1.0	.1	NACO	40	No
1072	4080AV	MTV	1.1	.1	NACO	40	No
1073	4080AV	MTV	1.2	.1	NACO	40	No
1074	4080AV	MTV	1.3	.1	NACO	40	Yes
1075	4080AV	MTV	1.2	.1	NACO	40	No
1076	4080AV	MTV	1.3	.1	NACO	40	No
1077	4080AV	MTV	1.4	.1	NACO	40	No
1078	4080AV	MTV	1.5	.1	NACO	40	No
1079	4080AV	MTV	1.6	.1	NACO	40	No
1080	4080AV	MTV	1.7	.1	NACO	40	No
1081	4080AV	MTV	1.8	.1	NACO	40	Yes
1082	4080AV	MTV	1.7	.1	NACO	40	No
1083	4080AV	MTV	1.8	.1	NACO	40	Yes
1084	4080AV	MTV	1.4	.2	NACO	40	No
1085	4080AV	MTV	1.6	.2	NACO	40	Yes
1086	4080AV	MTV	1.4	.2	NACO	40	No
1087	4080AV	MTV	1.6	.2	NACO	40	No
1088	4080AV	MTV	1.8	.2	NACO	40	Yes
1089	4080AV	MTV	1.6	.2	NACO	40	Yes
1090	4080AV	MTV	1.4	.2	NACO	40	No
1091	4080AV	MTV	1.6	.2	NACO	40	Yes
1092	4080AV	MTV	1.4	.2	NACO	40	No
1093	4080AV	MTV	1.6	.2	NACO	40	Yes
1094	4080AV	MTV	1.4	.2	NACO	40	No

APPENDIX B

Ignition Effectiveness Oscilloscope Data

Note: Symbols used in Data Log

* - No Data Record

> - (P_{2max}) Peak Off-scale

< - (t_{ign}) Primer pulse and propellant ignition merged

< - (t_{peak}) Peak off scale, time at last trace location

n/a - Primer only

Y - Yes, Propellant ignition did occur

N - No, Propellant ignition did not occur

INERT SIMULANT BED LENGTH - L_1 = 0.00 in

Test Number	Igniter Material	Igniter Mass (g)	Propellant (40g)	Ignition	P_{20} (psi)	P_{21} (psi)	P_{2max} (psi)	t_{ign} (msec)	t_{peak} (msec)
4001	n/a	n/a	LOVA	N	40	-	-	-	-
4002	n/a	n/a	LOVA	N	40	-	-	-	-
4003	BP	1.0	LOVA	N	220	-	-	-	-
4004	BP	1.5	LOVA	N	580	-	-	-	-
4005	BP	2.0	LOVA	N	750	-	-	-	-
4006	BP	2.0	LOVA	N	800	-	-	-	-
4007	BP	3.0	LOVA	N	1300	-	-	-	-
4008	BP	4.0	LOVA	Y	1950	1250	>4000	<20	<100
4009	BP	3.5	LOVA	Y	1700	1050	>4000	<20	<110
4010	BP	3.0	LOVA	Y	1300	450	2950	<30	<140
4011	BP	2.5	LOVA	N	1100	-	-	-	-
4012	BP	3.0	LOVA	Y	1300	550	3700	35	130
4013	BP	2.5	LOVA	N	*	*	*	*	*
4014	BP	2.8	LOVA	Y	1240	200	3700	50	150
4015	BP	2.5	LOVA	Y	1200	0	1300	100	20
4016	BP	2.2	LOVA	N	1000	-	-	-	-
4017	BP	2.5	LOVA	N	1150	-	-	-	-
4018	BP	2.8	LOVA	N	1230	-	-	-	-
4019	BP	3.1	LOVA	Y	1400	850	>4500	30	115
4020	BP	2.8	LOVA	N	1100	-	-	-	-
4021	BP	3.1	LOVA	Y	1400	850	>4500	25	100
4022	BP	2.8	LOVA	N	1300	-	-	-	-
4023	BP	3.1	LOVA	Y	1400	800	4950	30	110

*No Data Record

INERT SIMULANT BED LENGTH - L_1 = 0.00 in

Test Number	Igniter Material	Igniter Mass (g)	Propellant (40g)	Ignition	P_{20} (psi)	P_{21} (psi)	P_{2max} (psi)	t_{ign} (msec)	t_{peak} (msec)
4024	BKN	1.4	LOVA	N	1000	-	-	-	-
4025	BKN	1.7	LOVA	Y	1050	0	2200	35	140
4026	BKN	1.4	LOVA	N	800	-	-	-	-
4027	BKN	1.7	LOVA	Y	1000	0	2200	40	135
4028	BKN	1.4	LOVA	N	780	-	-	-	-
4029	BKN	1.6	LOVA	N	1000	-	-	-	-
4030	BKN	1.8	LOVA	Y	1200	500	5000	30	115
4031	BKN	1.6	LOVA	Y	1000	0	2000	50	150
4032	BKN	1.4	LOVA	N	800	-	-	-	-
4033	BKN	1.6	LOVA	Y	1000	400	4700	35	130
4034	BKN	1.4	LOVA	N	600	-	-	-	-
4035	BKN	1.6	LOVA	N	1000	-	-	-	-
4036	BKN	1.8	LOVA	Y	1100	200	2800	40	140
4037	BKN	1.6	LOVA	Y	800	300	4200	45	150
4038	BKN	1.4	LOVA	N	800	-	-	-	-

INERT SIMULANT BED LENGTH - L_1 = 0.00 in

Test Number	Igniter Material	Igniter Mass (g)	Propellant (40g)	Ignition	P_{20} (psi)	P_{21} (psi)	P_{2max} (psi)	t_{ign} (msec)	t_{peak} (msec)
4039	MTV	1.5	LOVA	N	600	-	-	-	-
4040	MTV	1.8	LOVA	Y	600	0	2800	45	135
4041	MTV	1.5	LOVA	N	600	-	-	-	-
4042	MTV	1.8	LOVA	Y	600	0	3400	50	140
4043	MTV	1.7	LOVA	N	650	-	-	-	-
4044	MTV	1.9	LOVA	Y	800	400	4900	35	120
4045	MTV	1.7	LOVA	N	700	-	-	-	-
4046	MTV	1.9	LOVA	Y	900	600	5400	35	120
4047	MTV	1.7	LOVA	Y	800	400	4800	50	150
4048	MTV	1.5	LOVA	N	800	-	-	-	-
4049	MTV	1.7	LOVA	Y	1000	1000	>8000	25	110
4050	MTV	1.5	LOVA	N	800	-	-	-	-
4051	MTV	1.7	LOVA	N	900	-	-	-	-
4052	MTV	1.9	LOVA	Y	1200	1200	>7000	25	110
4053	MTV	1.7	LOVA	Y	1000	900	5700	35	140

INERT SIMULANT BED LENGTH - L_1 = 0.00 in

Test Number	Igniter Material	Igniter Mass (g)	Propellant (40g)	Ignition	P_{20} (psi)	P_{21} (psi)	P_{2max} (psi)	t_{ign} (msec)	t_{peak} (msec)
4054	NC	2.2	LOVA	N	50	-	-	-	-
4055	NC	2.7	LOVA	N	100	-	-	-	-
4056	NC	3.2	LOVA	N	*	-	-	-	-
4057	NC	3.7	LOVA	Y	180	*	*	*	*
4058	NC	3.2	LOVA	N	180	-	-	-	-
4059	NC	3.7	LOVA	Y	180	0	4000	600	760
4060	NC	3.3	LOVA	Y	100	0	2600	450	650
4061	NC	2.9	LOVA	N	100	-	-	-	-
4062	NC	3.3	LOVA	N	200	-	-	-	-
4063	NC	3.7	LOVA	Y	180	0	>7000	800	960
4064	NC	3.3	LOVA	N	200	-	-	-	-
4065	NC	3.7	LOVA	Y	180	0	4500	630	800
4066	NC	3.3	LOVA	N	200	-	-	-	-
4067	NC	3.7	LOVA	N	200	-	-	-	-
4068	NC	4.1	LOVA	Y	200	0	>7000	460	590
4069	NC	3.7	LOVA	Y	200	0	6200	400	540

*No Data Record

INERT SIMULANT BED LENGTH - L_1 = 0.00 in

Test Number	Igniter Material	Igniter Mass (g)	Propellant (40g)	Ignition	P_{20} (psi)	P_{21} (psi)	P_{2max} (psi)	t_{ign} (msec)	t_{peak} (msec)
4111	BMoO	5.0	LOVA	N	80	-	-	-	-
4112	BMoO	6.0	LOVA	N	60	-	-	-	-
4113	BMoO	8.0	LOVA	N	20	-	-	-	-
4114	BMoO	10.0	LOVA	N	20	-	-	-	-
4115	BMoO	15.0	LOVA	N	*	*	*	*	*
4116	BMoO/NC	6.0/1.0	LOVA	N	100	-	-	-	-
4117	BMoO/NC	6.0/2.0	LOVA	N	70	-	-	-	-

*No Data Record

INERT SIMULANT BED LENGTH - L_1 = 0.00 in

Test Number	Igniter Material	Igniter Mass (g)	Propellant (40g)	Ignition	P_{20} (psi)	P_{21} (psi)	P_{2max} (psi)	t_{ign} (msec)	t_{peak} (msec)
4133	AP	2.0	LOVA	Y	500	0	>4000	30	95
4134	AP	1.0	LOVA	N	400	-	-	-	-
4135	AP	1.5	LOVA	Y	500	400	4950	5	108
4136	AP	1.3	LOVA	Y	800	0	3300	40	125
4137	AP	1.1	LOVA	N	250	-	-	-	-
4138	AP	1.3	LOVA	Y	600	400	7200	8	125
4139	AP	1.1	LOVA	N	200	-	-	-	-
4140	AP	1.3	LOVA	Y	500	350	1600	10	120
4141	AP	1.1	LOVA	N	200	-	-	-	-
4142	AP	1.3	LOVA	N	500	-	-	-	-
4143	AP	1.5	LOVA	Y	800	600	1400	5	135
4144	AP	1.3	LOVA	Y	500	300	1200	10	155
4145	AP	1.1	LOVA	N	450	-	-	-	-
4146	AP	1.3	LOVA	Y	500	0	4200	25	145

INERT SIMULANT BED LENGTH - L_1 = 1.00 in

Test Number	Igniter Material	Igniter Mass (g)	Propellant (40g)	Ignition	P_{20} (psi)	P_{21} (psi)	P_{2max} (psi)	t_{ign} (msec)	t_{peak} (msec)
173	n/a	n/a	NACO	n/a	n/a	n/a	n/a	n/a	n/a
174	BP	1.0	NACO	Y	50	0	>4000	1700	1950
175	BP	0.7	NACO	N	30	-	-	-	-
176	BP	1.0	NACO	N	200	-	-	-	-
177	BP	1.3	NACO	N	200	-	-	-	-
178	BP	1.6	NACO	Y	650	0	>4000	1600	1750
179	BP	1.3	NACO	N	250	-	-	-	-
180	BP	1.6	NACO	Y	400	0	>4000	2000	2100
181	BP	1.3	NACO	Y	580	0	>4000	2400	2500
182	BP	1.0	NACO	N	150	-	-	-	-
183	BP	1.3	NACO	Y	500	0	>4000	2500	2630
184	BP	1.0	NACO	N	420	-	-	-	-
185	BP	1.3	NACO	Y	600	0	>4000	1700	1820

INERT SIMULANT BED LENGTH - L_1 = 1.00 in

Test Number	Igniter Material	Igniter Mass (g)	Propellant (40g)	Ignition	P_{20} (psi)	P_{21} (psi)	P_{2max} (psi)	t_{ign} (msec)	t_{peak} (msec)
186	BKN	0.6	NACO	N	130	-	-	-	-
187	BKN	0.7	NACO	Y	130	0	>4000	2300	2450
188	BKN	0.6	NACO	N	130	-	-	-	-
189	BKN	0.7	NACO	Y	190	0	>4000	2100	2220
190	BKN	0.6	NACO	N	130	-	-	-	-
191	BKN	0.7	NACO	Y	150	0	>4000	1900	2050
192	BKN	0.6	NACO	N	100	-	-	-	-
193	BKN	0.7	NACO	N	200	-	-	-	-
194	BKN	0.8	NACO	Y	210	0	>4000	2000	2150
195	BKN	0.7	NACO	Y	180	0	>4000	1850	2000
196	BKN	0.6	NACO	N	150	-	-	-	-

INERT SIMULANT BED LENGTH - L_1 = 1.00 in

Test Number	Igniter Material	Igniter Mass (g)	Propellant (40g)	Ignition	P_{20} (psi)	P_{21} (psi)	P_{2max} (psi)	t_{ign} (msec)	t_{peak} (msec)
1001	NC	2.0	NACO	Y	30	0	>4000	1750	1850
1002	NC	1.5	NACO	N	30	-	-	-	-
1003	NC	2.0	NACO	Y	30	0	>4000	2200	2370
1004	NC	1.8	NACO	Y	25	0	>4000	2500	2620
1005	NC	1.6	NACO	Y	80	0	>4000	1650	1900
1006	NC	1.4	NACO	Y	25	*	*	4000	*
1007	NC	1.2	NACO	Y	20	0	>4000	2300	2500
1008	NC	1.0	NACO	N	40	-	-	-	-
1009	NC	1.2	NACO	N	25	-	-	-	-
1010	NC	1.2	NACO	Y	25	0	>4000	2100	2220
1011	NC	1.0	NACO	N	25	-	-	-	-
1012	NC	1.2	NACO	Y	40	0	>4000	2600	2730
1013	NC	1.0	NACO	N	20	-	-	-	-
1014	NC	1.2	NACO	N	*	-	-	-	-
1015	NC	1.2	NACO	N	*	-	-	-	-
1016	NC	1.2	NACO	Y	40	0	>4000	2100	2250
1017	NC	1.0	NACO	N	20	-	-	-	-
1018	NC	1.2	NACO	Y	25	0	3500	3050	3250
1019	NC	1.0	NACO	N	20	-	-	-	-
1020	NC	1.2	NACO	N	20	-	-	-	-
1021	NC	1.2	NACO	Y	20	0	>4000	3450	3600

*No Data Record

INERT SIMULANT BED LENGTH - L_1 = 1.00 in

Test Number	Igniter Material	Igniter Mass (g)	Propellant (40g)	Ignition	P_{20} (psi)	P_{21} (psi)	P_{2max} (psi)	t_{ign} (msec)	t_{peak} (msec)
1095	BMO	4.0	NACO	N	50	-	-	-	-
1096	BMO	4.5	NACO	Y	25	0	2580	2750	2900
1097	BMO	4.0	NACO	Y	25	0	*	5000	*
1098	BMO	3.5	NACO	N	25	-	-	-	-
1099	BMO	4.0	NACO	Y	25	*	*	>4500	*
1100	BMO	3.5	NACO	Y	*	*	*	*	*
1101	BMO	3.0	NACO	N	25	-	-	-	-
1102	BMO	3.5	NACO	N	25	-	-	-	-
1103	BMO	4.0	NACO	Y	25	0	>4000	2200	2350
1104	BMO	3.5	NACO	Y	25	0	3600	2700	2800
1105	BMO	3.0	NACO	N	*	-	-	-	-

*No Data Record

INERT SIMULANT BED LENGTH - L_1 = 1.00 in

Test Number	Igniter Material	Igniter Mass (g)	Propellant (40g)	Ignition	P_{20} (psi)	P_{21} (psi)	P_{2max} (psi)	t_{ign} (msec)	t_{peak} (msec)
2001	BKN	1.4	N318	Y	350	0	*	10000	10C00
2002	BKN	1.2	N318	N	320	-	-	-	-
2003	BKN	1.4	N318	N	400	-	-	-	-
2004	BKN	1.6	N318	N	600	-	-	-	-
2005	BKN	1.8	N318	N	550	-	-	-	-
2006	BKN	2.0	N318	N	700	-	-	-	-
2007	BKN	2.2	N318	Y	950	0	2400	5000	5000
2008	BKN	2.0	N318	Y	740	0	930	8600	8800
2009	BKN	1.8	N318	Y	500	0	2000	6000	6200
2010	BKN	1.6	N318	N	500	-	-	-	-
2011	BKN	1.8	N318	N	630	-	-	-	-
2012	BKN	2.0	N318	Y	840	0	2500	8300	8500
2013	BKN	1.8	N318	N	710	-	-	-	-
2014	BKN	2.0	N318	Y	800	0	1950	6700	6900

*No Data Record

INERT SIMULANT BED LENGTH - L_1 = 1.00 in

Test Number	Igniter Material	Igniter Mass (g)	Propellant (40g)	Ignition	P_{20} (psi)	P_{21} (psi)	P_{2max} (psi)	t_{ign} (msec)	t_{peak} (msec)
2015	NC	2.3	N318	Y	80	*	*	5000	*
2016	NC	2.0	N318	Y	120	0	1700	7250	7380
2017	NC	1.7	N318	Y	70	0	120	9000	11800
2018	NC	1.4	N318	N	50	-	-	-	-
2019	NC	1.7	N318	Y	60	0	1000	8500	11600
2020	NC	1.4	N318	N	100	-	-	-	-
2021	NC	1.7	N318	Y	100	0	1520	11000	13200
2022	NC	1.4	N318	Y	80	0	1850	10500	12800
2023	NC	1.1	N318	Y	*	*	*	≈5000	*
2024	NC	0.9	N318	N	80	-	-	-	-
2025	NC	1.1	N318	N	90	-	-	-	-
2026	NC	1.4	N318	Y	60	0	1500	9500	11000
2027	NC	1.1	N318	N	70	-	-	-	-

*No Data Record

INERT SIMULANT BED LENGTH - L_1 = 1.00 in

Test Number	Igniter Material	Igniter Mass (g)	Propellant (40g)	Ignition	P_{20} (psi)	P_{21} (psi)	P_{2max} (psi)	t_{ign} (msec)	t_{peak} (msec)
4085	BP	3.5	LOVA	N	1020	-	-	-	-
4086	BP	4.0	LOVA	Y	1300	0	650	<100	<150
4087	BP	3.5	LOVA	N	1080	-	-	-	-
4088	BP	4.0	LOVA	Y	1500	600	4400	20	80
4089	BP	3.5	LOVA	N	1100	-	-	-	-
4090	BP	3.8	LOVA	N	1200	-	-	-	-
4091	BP	4.1	LOVA	Y	1350	750	2300	20	95
4092	BP	3.8	LOVA	N	1250	-	-	-	-
4093	BP	4.1	LOVA	N	1500	-	-	-	-
4094	BP	4.4	LOVA	Y	1500	0	1300	35	140
4095	BP	4.1	LOVA	Y	1400	150	1500	25	105
4096	BP	3.8	LOVA	N	1380	-	-	-	-
4097	BP	4.1	LOVA	Y	1400	600	6900	15	75
4098	BP	3.8	LOVA	N	1450	-	-	-	-
4099	BP	4.1	LOVA	N	1300	-	-	-	-

INERT SIMULANT BED LENGTH - L_1 = 1.00 in

Test Number	Igniter Material	Igniter Mass (g)	Propellant (40g)	Ignition	P_{20} (psi)	P_{21} (psi)	P_{2max} (psi)	t_{ign} (msec)	t_{peak} (msec)
4100	BKN	2.4	LOVA	Y	1250	0	1300	*	*
4101	BKN	2.1	LOVA	N	1000	-	-	-	-
4102	BKN	2.4	LOVA	Y	1250	500	2200	25	125
4103	BKN	2.1	LOVA	Y	950	0	1200	40	155
4104	BKN	1.8	LOVA	N	600	-	-	-	-
4105	BKN	2.1	LOVA	N	950	-	-	-	-
4106	BKN	2.4	LOVA	Y	1200	500	1900	20	105
4107	BKN	2.1	LOVA	Y	1000	0	1650	35	135
4108	BKN	1.8	LOVA	N	800	-	-	-	-
4109	BKN	2.1	LOVA	Y	1000	200	1750	45	165
4110	BKN	1.8	LOVA	N	700	-	-	-	-

*No Data Record

INERT SIMULANT BED LENGTH - L_1 = 1.00 in

Test Number	Igniter Material	Igniter Mass (g)	Propellant (40g)	Ignition	P_{20} (psi)	P_{21} (psi)	P_{2max} (psi)	t_{ign} (msec)	t_{peak} (msec)
4118	MTV	2.0	LOVA	N	650	-	-	-	-
4119	MTV	2.3	LOVA	Y	700	0	2750	≈30	130
4120	MTV	2.0	LOVA	N	500	-	-	-	-
4121	MTV	2.3	LOVA	Y	500	0	2200	35	130
4122	MTV	2.0	LOVA	Y	400	0	1600	55	160
4123	MTV	1.8	LOVA	N	500	-	-	-	-
4124	MTV	2.0	LOVA	Y	650	0	2300	60	160
4125	MTV	1.8	LOVA	N	500	-	-	-	-
4126	MTV	2.0	LOVA	Y	600	0	3200	45	150
4127	MTV	1.8	LOVA	N	600	-	-	-	-
4128	MTV	2.0	LOVA	Y	600	0	≈5000	40	135
4129	MTV	1.8	LOVA	N	450	-	-	-	-
4130	MTV	2.0	LOVA	N	650	-	-	-	-
4131	MTV	2.2	LOVA	Y	750	0	2800	40	140
4132	MTV	2.0	LOVA	N	600	-	-	-	-

INERT SIMULANT BED LENGTH - L_1 = 1.50 in

Test Number	Igniter Material	Igniter Mass (g)	Propellant (40g)	Ignition	P_{20} (psi)	P_{21} (psi)	P_{2max} (psi)	t_{ign} (msec)	t_{peak} (msec)
4070	NC	3.0	PYRO	N	25	-	-	-	-
4071	NC	3.5	PYRO	N	25	-	-	-	-
4072	NC	4.0	PYRO	Y	100	0	>4000	340	400
4073	NC	3.5	PYRO	N	25	-	-	-	-
4074	NC	4.0	PYRO	Y	100	0	9200	480	530
4075	NC	3.6	PYRO	Y	100	0	7900	<10	<30
4076	NC	3.2	PYRO	Y	100	0	8600	<10	<40
4077	NC	2.8	PYRO	N	100	-	-	-	-
4078	NC	3.2	PYRO	Y	100	0	6700	520	530
4079	NC	2.8	PYRO	N	100	-	-	-	-
4080	NC	3.2	PYRO	Y	100	0	9500	<10	<30
4081	NC	2.8	PYRO	N	100	-	-	-	-
4082	NC	3.2	PYRO	Y	150	0	11000	35	390
4083	NC	2.8	PYRO	N	100	-	-	-	-
4084	NC	3.2	PYRO	N	100	-	-	-	-

INERT SIMULANT BED LENGTH - L_1 = 1.50 in

Test Number	Igniter Material	Igniter Mass (g)	Propellant (40g)	Ignition	P_{20} (psi)	P_{21} (psi)	P_{2max} (psi)	t_{ign} (msec)	t_{peak} (msec)
4147	AP	2.5	LOVA	N	1000	-	-	-	-
4148	AP	2.8	LOVA	N	500	-	-	-	-
4149	AP	3.1	LOVA	Y	1000	1000	3300	5	80
4150	AP	2.8	LOVA	Y	400	0	3800	15	115
4151	AP	2.5	LOVA	N	250	-	-	-	-
4152	AP	2.8	LOVA	Y	1200	1200	1500	3	115
4153	AP	2.5	LOVA	Y	1100	1100	2100	3	110
4154	AP	2.2	LOVA	N	600	-	-	-	-
4155	AP	2.5	LOVA	Y	450	0	2000	15	145
4156	AP	2.2	LOVA	N	300	-	-	-	-
4157	AP	2.5	LOVA	Y	600	500	2400	5	138
4158	AP	2.2	LOVA	Y	1400	1200	4200	8	110
4159	AP	1.3	LOVA	N	200	-	-	-	-

INERT SIMULANT BED LENGTH - L_2 = 2.00 in

Test Number	Igniter Material	Igniter Mass (g)	Propellant (40g)	Ignition	P_{20} (psi)	P_{21} (psi)	P_{2max} (psi)	t_{ign} (msec)	t_{peak} (msec)
1022	BP	2.2	NACO	N	320	-	-	-	-
1023	BP	2.6	NACO	N	540	-	-	-	-
1024	BP	3.0	NACO	N	700	-	-	-	-
1025	BP	3.4	NACO	Y	800	540	>4000	<40	60
1026	BP	3.0	NACO	Y	610	0	>4000	3750	3810
1027	BP	2.6	NACO	N	490	-	-	-	-
1028	BP	3.0	NACO	Y	700	0	>4000	1650	1800
1029	BP	2.8	NACO	Y	610	0	>4000	2100	2270
1030	BP	2.6	NACO	Y	550	0	>4000	3940	4080
1031	BP	2.4	NACO	N	440	-	-	-	-
1032	BP	2.6	NACO	N	540	-	-	-	-
1033	BP	2.8	NACO	N	500	-	-	-	-
1034	BP	3.0	NACO	Y	600	0	>4000	1800	1950
1035	BP	2.8	NACO	N	570	-	-	-	-
1036	BP	3.0	NACO	Y	800	580	>4000	20	60
1037	BP	2.8	NACO	N	590	-	-	-	-
1038	BP	3.0	NACO	N	650	-	-	-	-

INERT SIMULANT BED LENGTH - L_2 = 2.00 in

Test Number	Igniter Material	Igniter Mass (g)	Propellant (40g)	Ignition	P_{20} (psi)	P_{21} (psi)	P_{2max} (psi)	t_{ign} (msec)	t_{peak} (msec)
1039	BKN	1.2	NACO	Y	250	0	>4000	1780	1900
1040	BKN	1.0	NACO	N	120	-	-	-	-
1041	BKN	1.2	NACO	Y	200	0	>4000	2250	2380
1042	BKN	1.1	NACO	N	210	-	-	-	-
1043	BKN	1.2	NACO	Y	170	0	>4000	1650	1780
1044	BKN	1.1	NACO	N	170	-	-	-	-
1045	BKN	1.2	NACO	Y	*	0	>4000	1720	1900
1046	BKN	1.1	NACO	Y	*	0	>4000	2080	2200
1047	BKN	1.0	NACO	Y	200	0	>4000	1930	2060
1048	BKN	0.9	NACO	N	130	-	-	-	-
1049	BKN	1.0	NACO	N	200	-	-	-	-
1050	BKN	1.1	NACO	Y	170	0	1100	1800	2040
1051	BKN	1.0	NACO	Y	160	0	3500	3900	3100

*No Data Record

INERT SIMULANT BED LENGTH - L_2 = 2.00 in

Test Number	Igniter Material	Igniter Mass (g)	Propellant (40g)	Ignition	P_{20} (psi)	P_{21} (psi)	P_{2max} (psi)	t_{ign} (msec)	t_{peak} (msec)
1052	NC	2.0	NACO	N	90	-	-	-	-
1053	NC	2.5	NACO	N	110	-	-	-	-
1054	NC	3.0	NACO	N	100	-	-	-	-
1055	NC	3.5	NACO	Y	200	200	>4000	20	40
1056	NC	3.0	NACO	Y	150	50	>4000	20	40
1057	NC	2.5	NACO	Y	100	100	>4000	20	60
1058	NC	2.0	NACO	N	100	-	-	-	-
1059	NC	2.5	NACO	N	50	-	-	-	-
1060	NC	3.0	NACO	Y	190	50	>4000	20	50
1061	NC	2.5	NACO	N	110	-	-	-	-
1062	NC	3.0	NACO	N	100	-	-	-	-
1063	NC	3.5	NACO	Y	*	*	*	*	*

*No Data Record

INERT SIMULANT BED LENGTH - L_1 = 2.00 in

Test Number	Igniter Material	Igniter Mass (g)	Propellant (40g)	Ignition	P_{20} (psi)	P_{21} (psi)	P_{2max} (psi)	t_{ign} (msec)	t_{peak} (msec)
1064	MTV	1.2	NACO	N	150	-	-	-	-
1065	MTV	1.4	NACO	Y	220	0	*	2200	*
1066	MTV	1.2	NACO	Y	180	0	>4000	3150	3300
1067	MTV	1.0	NACO	Y	200	0	>4000	3600	2750
1068	MTV	0.9	NACO	N	120	-	-	-	-
1069	MTV	1.0	NACO	N	200	-	-	-	-
1070	MTV	1.1	NACO	Y	150	0	>4000	3300	3500
1071	MTV	1.0	NACO	N	160	-	-	-	-
1072	MTV	1.1	NACO	N	140	-	-	-	-
1073	MTV	1.2	NACO	N	200	-	-	-	-
1074	MTV	1.3	NACO	Y	250	0	*	4500	*
1075	MTV	1.2	NACO	N	120	-	-	-	-
1076	MTV	1.3	NACO	N	260	-	-	-	-
1077	MTV	1.4	NACO	N	250	-	-	-	-
1078	MTV	1.5	NACO	N	240	-	-	-	-
1079	MTV	1.6	NACO	N	340	-	-	-	-
1080	MTV	1.7	NACO	N	320	-	-	-	-
1081	MTV	1.8	NACO	Y	460	0	>4000	2250	2410
1082	MTV	1.7	NACO	N	350	-	-	-	-
1083	MTV	1.8	NACO	Y	450	0	2900	2100	2230
1084	MTV	1.4	NACO	N	250	-	-	-	-
1085	MTV	1.6	NACO	Y	250	0	>4000	2600	2710
1086	MTV	1.4	NACO	N	260	-	-	-	-
1087	MTV	1.6	NACO	N	250	-	-	-	-
1088	MTV	1.8	NACO	Y	360	30	>4000	60	100
1089	MTV	1.6	NACO	Y	400	0	>4000	2200	2370
1090	MTV	1.4	NACO	N	300	-	-	-	-
1091	MTV	1.6	NACO	Y	320	0	>4000	80	110
1092	MTV	1.4	NACO	N	280	-	-	-	-
1093	MTV	1.6	NACO	Y	350	0	>4000	1600	1730
1094	MTV	1.4	NACO	N	220	-	-	-	-

*No Data Record

APPENDIX C

Corrected Zone 2 Input Energy as a Function of Igniter Mass: Working Curves

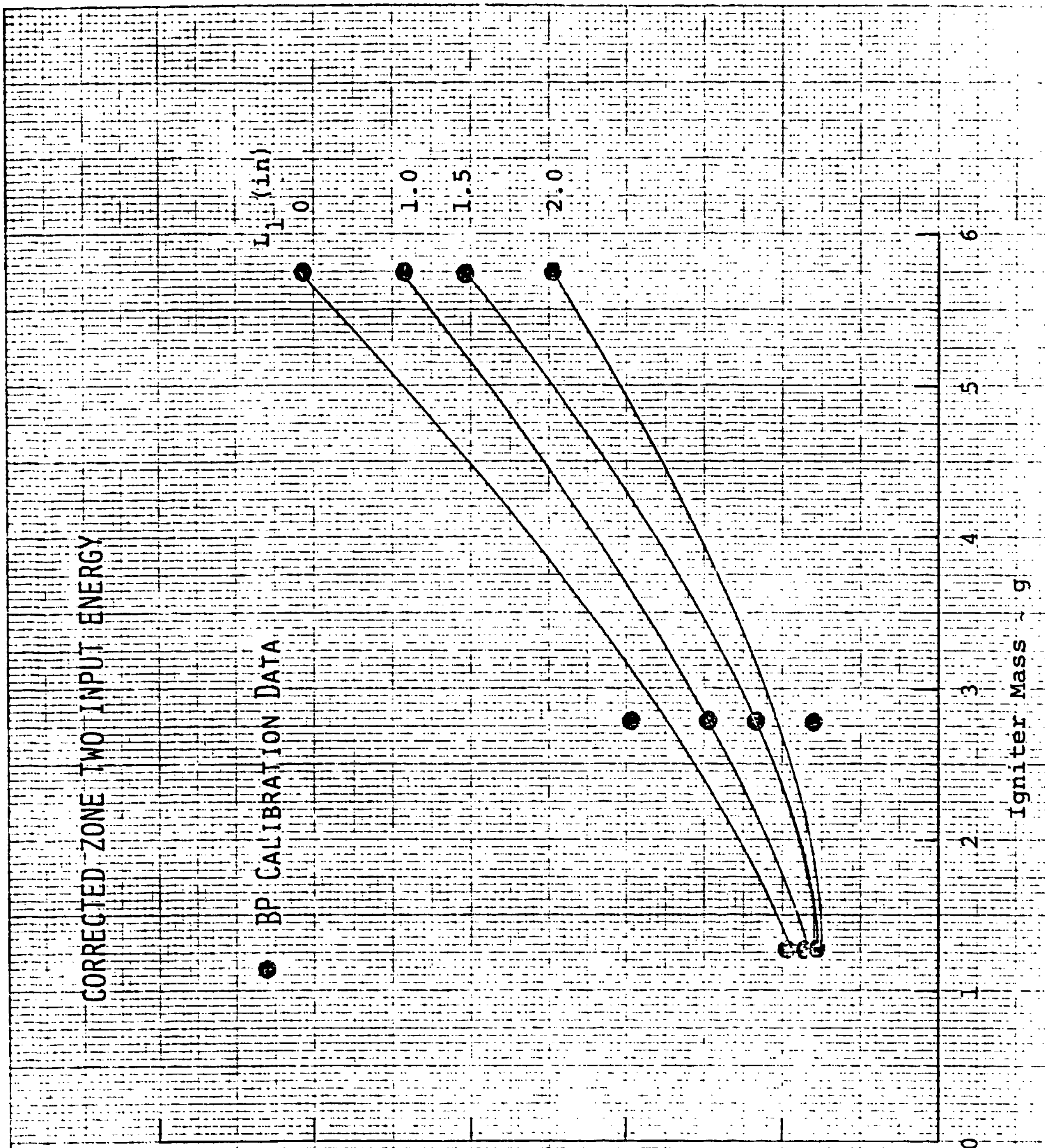

Figure C.1 Corrected Zone Two Input Energy: BP Calibration Data

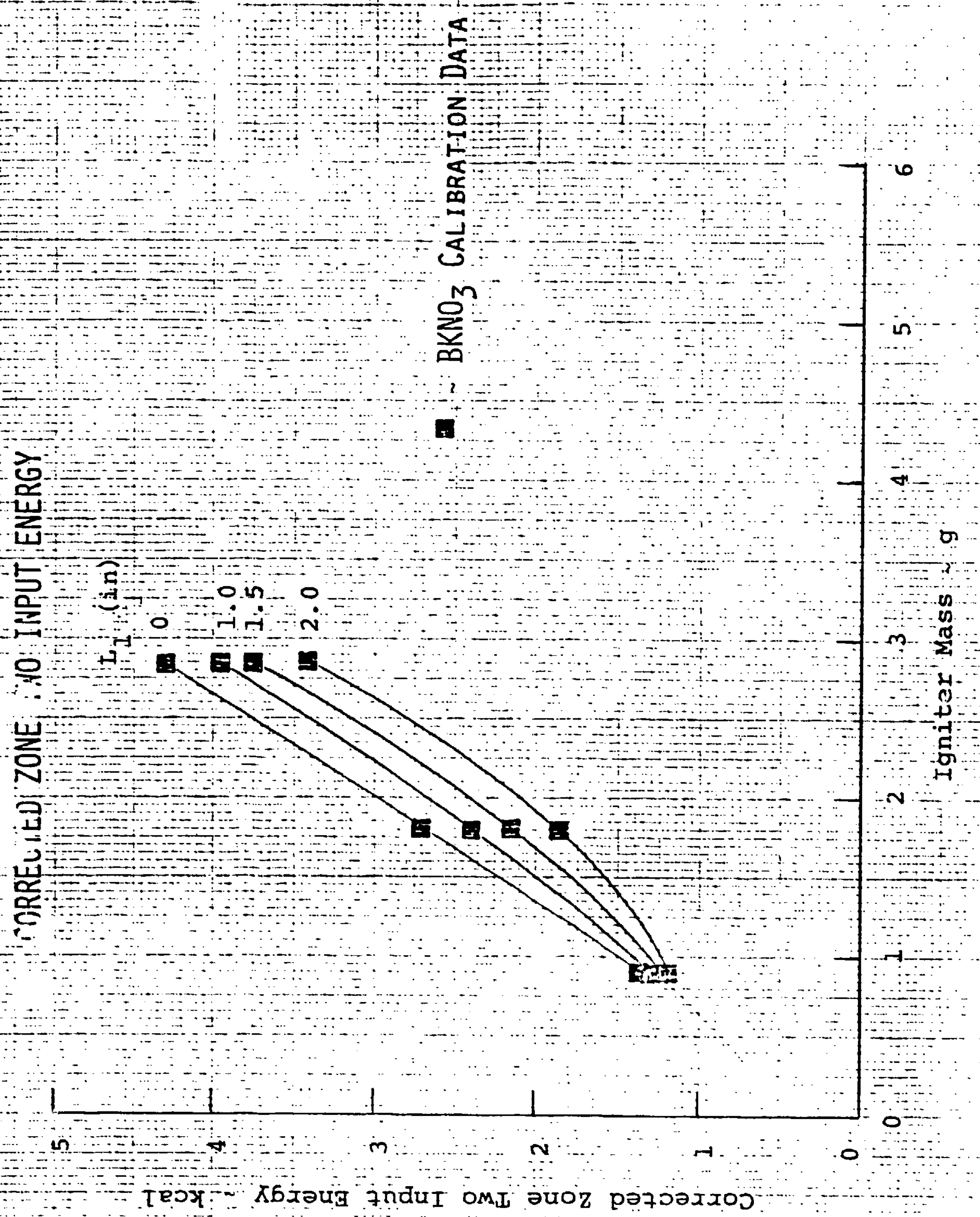

Figure C.2 Corrected Zone Two Input Energy: $BKNO_3$ Calibration Data

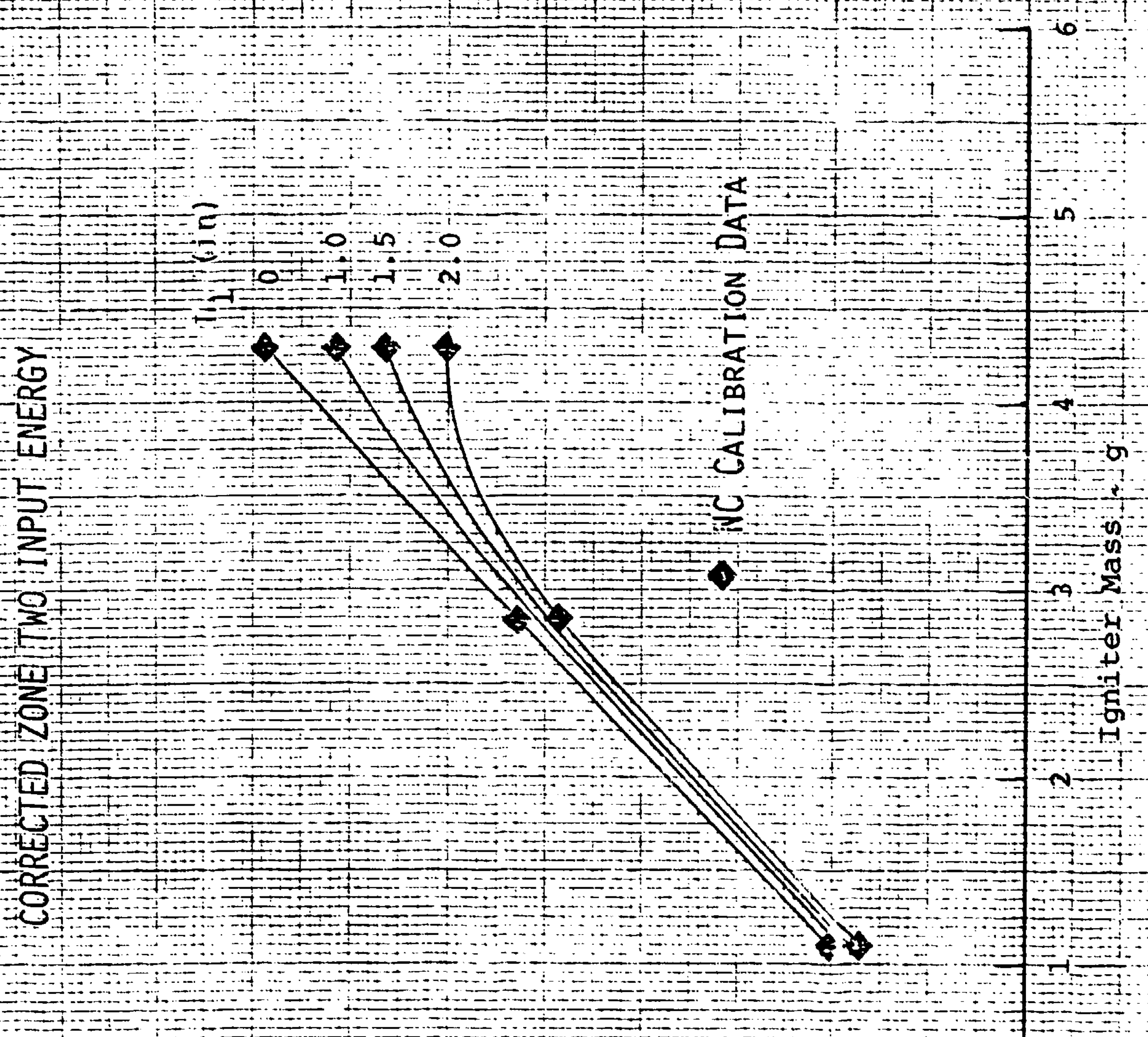

Figure C.3 Corrected Zone Two Input Energy: NC Calibration Data

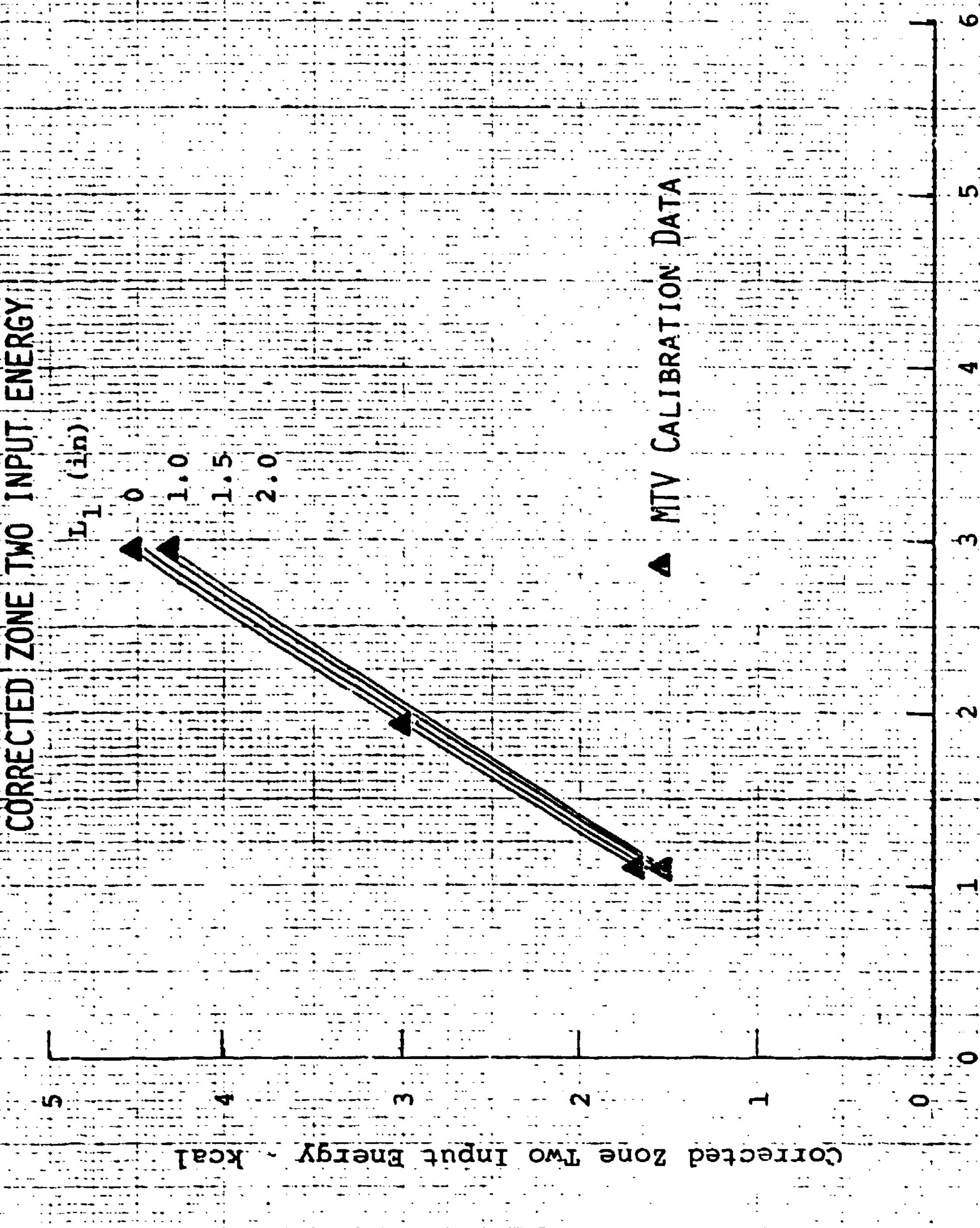

Figure C.4 Corrected Zone Two Input Energy: MTV Calibration Data

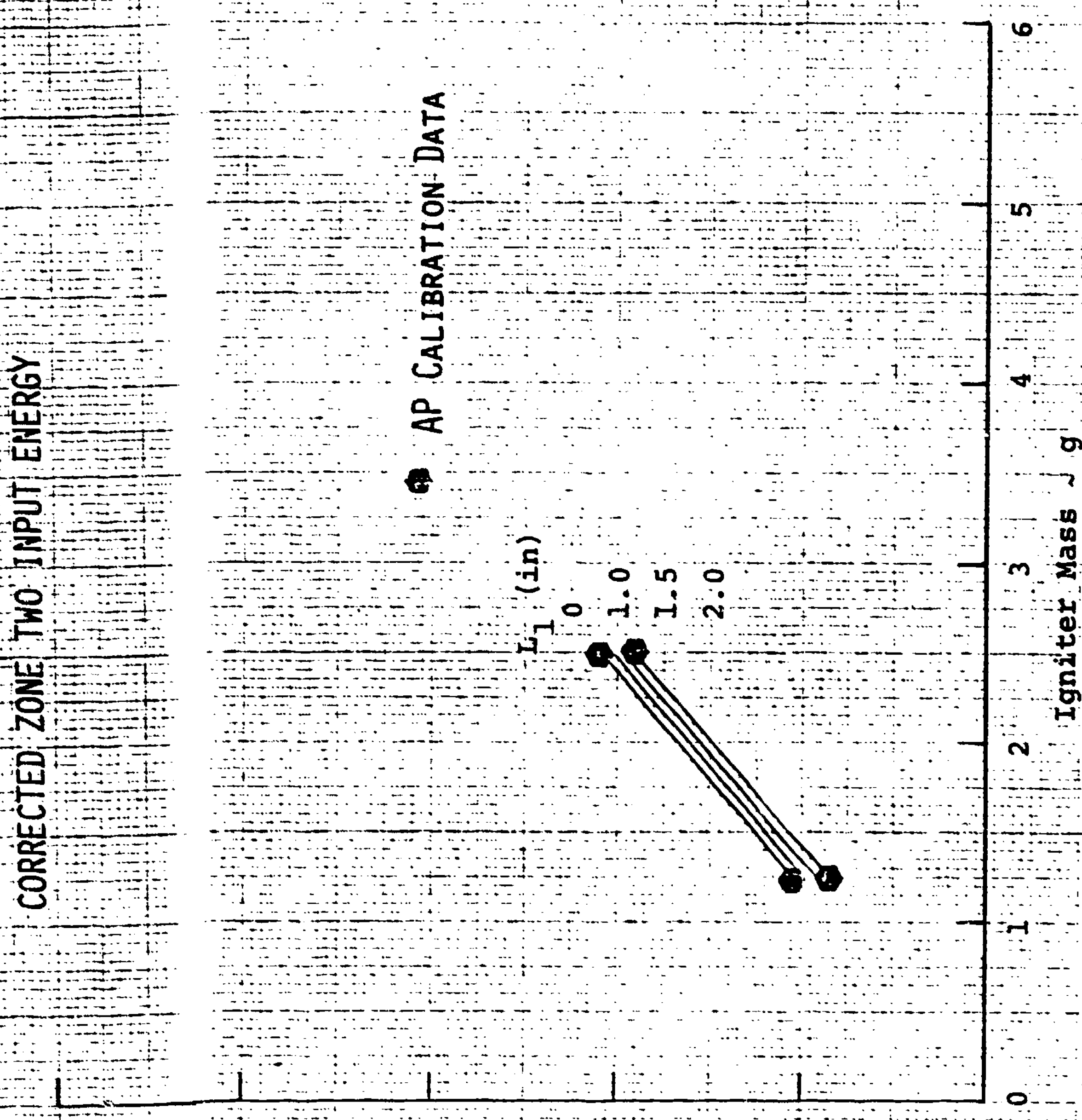

Figure C.5 Corrected Zone Two Input Energy: AP Calibration Data